REVIEW ARTICLE

Electrochemical reduction of gaseous nitric oxide into ammonia: a review

Jayaraman Theerthagiri[1] · K. Karuppasamy[2,7] · Abdul Hanif Mahadi[3] · Cheol Joo Moon[1] · Nihila Rahamathulla[4] · Soorathep Kheawhom[5] · Saeed Alameri[2,7] · Akram Alfantazi[6,7] · Arun Prasad Murthy[4] · Myong Yong Choi[1]

Abstract
Electrochemical reduction of gaseous nitric oxide gas is an appealing approach for simultaneously recycling nitric oxide and producing value-added ammonia. Indeed, ammonia finds applications in fertilizers production for agriculture, as a reagent in the pharmaceutical, explosive, and textile industries, and as a potential fuel for next-generation automotive fuel cells. Reduction of nitric oxide to ammonia using various electrode materials in electrochemical processes is reviewed. Materials primarily fall into two major categories: metal-based catalysts and carbon-supported catalysts. The key consideration and operational analysis to understand mechanistic reaction pathways and the selective production of product and intermediate are discussed from a prospective viewpoint.

Keywords Electrochemical reduction reaction · Nitric oxide gas · Waste-to-value-added chemicals · Ammonia · Electrocatalysis

Introduction

Nitric oxide (NO) is a major air pollutant that severely threatens both the environment and human beings. Limiting the emission of NO gas is imperative, as it is abundantly produced through the continual, excessive combustion of fossil fuels in power plants, industries, and automobiles. Furthermore, NO contributes to respiratory issues, acid rain, and ozone layer depletion. When NO reacts with atmospheric oxygen, it forms nitrogen oxide (NO_2), which can further react with hydroxyl radicals to produce nitic acid (HNO_3), resulting in acid rains and greenhouse gases (Soto-Hernández et al. 2019; Wang et al. 2023). Finding an alternative and environmentally friendly approach for NO removal is crucial, as previous research has suggested adsorption and catalysis as potential methods to eliminate NO. Selective catalytic reduction is a promising catalysis method for NO removal, although the requirement for a reducing agent complicates the procedure (Li et al. 2023;

Jayaraman Theerthagiri, K. Karuppasamy, Abdul Hanif Mahadi, Cheol Joo Moon and Nihila Rahamathulla have contributed equally to this work.

✉ Akram Alfantazi
akram.alfantazi@ku.ac.ae

✉ Arun Prasad Murthy
arunprasad.m@vit.ac.in

✉ Myong Yong Choi
mychoi@gnu.ac.kr

1   Core-Facility Center for Photochemistry and Nanomaterials, Department of Chemistry (BK21 FOUR), Research Institute of Natural Science, Gyeongsang National University, Jinju 52828, Republic of Korea

2   Department of Mechanical and Nuclear Engineering, Khalifa University of Science and Technology, 127788, Abu Dhabi, United Arab Emirates

3   Centre of Advanced Material and Energy Sciences, Universiti Brunei Darussalam, Jalan Tungku Link, Bandar Seri Begawan, BE 1410, Brunei Darussalam

4   Department of Chemistry, School of Advanced Sciences, Vellore Institute of Technology, Vellore, Tamil Nadu 632014, India

5   Department of Chemical Engineering, Faculty of Engineering, Chulalongkorn University, Bangkok 10330, Thailand

6   Department of Chemical and Petroleum Engineering, Khalifa University of Science and Technology, 127788, Abu Dhabi, United Arab Emirates

7   Emirates Nuclear Technology Center (ENTC), Khalifa University of Science and Technology, 127788, Abu Dhabi, United Arab Emirates

Soto-Hernández et al. 2019; Theerthagiri et al. 2022a). Therefore, finding an affordable and environmentally friendly alternative for NO removal is of utmost importance.

Artificial nitrogen cycle fixation offers a more energy-efficient approach by reducing nitrogen-containing compounds, such as nitrogen (N_2), nitrate (NO_3^-), and NO, instead of relying on high-energy-consuming processes (Dorado et al. 2007; Lang et al. 2020; Shahid et al. 2021). Additionally, converting NO pollutants into valuable nitrogenous compounds, such as ammonia (NH_3), N_2, nitrous oxide (N_2O), and hydroxylamine (NH_2OH), can help mitigate the effects of NO and balance the nitrogen cycle (Kim et al. 2021). Electrochemical reduction of NO is more favorable than electrochemical N_2 reduction owing to greater solubility, more nucleophilic nature, and lower bond energy of N=O (204 kJ mol^{-1}), whereas N≡N bond energy is 941 kJ mol^{-1} at 298 K (Chen et al. 2023a; Fan et al. 2023; Theerthagiri et al. 2022b; Wu et al. 2021b). In addition, the NO reduction reaction is thermodynamically more feasible than the N_2 reduction reaction, exhibits better selectivity and energy efficiency, and can be carried out under standard temperature conditions solely driven by applied potential, unlike the energy-intensive Haber–Bosch process for NH_3 production (Chen et al. 2023b; Jiang et al. 2022; Long et al. 2023; Wu et al. 2021b).
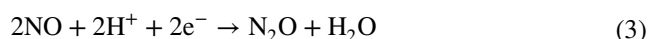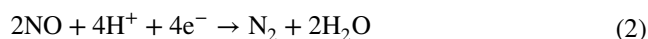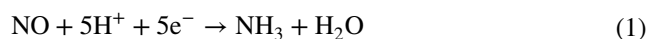
However, the electrochemical reduction of NO presents challenges related to the control of nitrogenous compounds, complicated reaction mechanisms, false positive conversions by other nitrogen-containing intermediates, solubility control of NO, maximizing Faradaic efficiency by eliminating competitive hydrogen evolution reaction, product separation, catalyst stability, and electrode durability (Kwon et al. 2021; Shahid et al. 2021; Shrestha et al. 2018).

These challenges need to be addressed to achieve the production of NH_3 with appreciable Faradaic efficiency. Herein, we review the electrochemical reduction of NO, emphasizing the mechanistic pathways, electrocatalysts, and selective NH_3 production in higher yields. We delve into the details of the rationally designed catalysts and electrode materials that exhibit improved electrochemical activity and selectivity in NH_3 production. Furthermore, the difficulties and possibilities related to this subject are discussed.
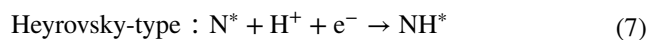
Mechanism of electrochemical reduction of nitric oxide

Long et al. (2021) conducted mechanistic studies on the NO reduction reaction using various transition metals, revealing a NO reduction reaction potential dependence on selective product formation. Specifically, NH_3 production was observed in a low potential range of 0–0.3 V versus the standard hydrogen electrode, N_2 was formed in a moderate potential of 0.2–0.4 V versus standard hydrogen electrode, and N_2O was generated at

a high potential range of 0.4–0.7 V versus standard hydrogen electrode (Wan et al. 2021). The reduction reactions occurring at various potential ranges are depicted in Eqs. (1–3). Wang et al. (2018) showed the importance of the adsorption mode of NO on the catalyst, which is another crucial description for product selectivity. When oxygen-end of NO adsorption occurs facilitating the coupling of the N–N bond, N_2O formation succeeds. Conversely, nitrogen-end NO adsorption results in NH_3 formation. Moreover, in an acidic electrolyte, the preferential formation of NH_3 over N_2 is observed (Ko et al. 2022).

$$NO + 5H^+ + 5e^- \rightarrow NH_3 + H_2O \tag{1}$$

$$2NO + 4H^+ + 4e^- \rightarrow N_2 + 2H_2O \tag{2}$$

$$2NO + 2H^+ + 2e^- \rightarrow N_2O + H_2O \tag{3}$$

Two main mechanisms for the NO reduction reaction have been proposed: the dissociative and associative mechanisms. In the dissociative mechanism, after NO adsorption on the surface of the catalysts, the N–O bond dissociates into nitrogen (*N) and oxygen (*O) atoms, followed by protonation to produce NH_3. However, the direct thermochemical dissociation of N–O faces several energy barriers (He et al. 2022a, b; Wu et al. 2021b). In addition, the hydrogenation required for the NO reduction reaction is governed by the hydrogen evolution reaction. During the NO reduction reaction, hydrogenation mainly proceeds via Tafel-mediated or Heyrovsky-mediated pathways, involving adsorbed *H adatoms. These adatoms are produced either by solvated protons adsorbed on the surface of the catalyst, forming H*, or via H$^+$ as a hydrogen source (Long et al. 2020). The reactions involving the Tafel-mediated pathway or Heyrovsky-mediated pathway are demonstrated in Eqs. (5–7). The dissociation of NO* into N* and O* adatoms requires 2.87 eV, as given in Eq. (4) (Long et al. 2021). The subsequent hydrogenation of NH* intermediate results in the final product NH_3, as illustrated in Eqs. (8) and (9).

$$NO(g) \rightarrow N^* + O^* \tag{4}$$

$$\text{Tafel-type} : H^+ + e^- \rightarrow H^* \tag{5}$$

$$N^* + H^* \rightarrow NH^* \tag{6}$$

$$\text{Heyrovsky-type} : N^* + H^+ + e^- \rightarrow NH^* \tag{7}$$

$$NH^* + H^* \rightarrow NH_2^* \tag{8}$$

$$NH_2^* + H^* \rightarrow NH_3 \tag{9}$$

In the associative mechanism, NO molecules are adsorbed onto the catalyst surface without breaking the N–O bond and

subsequent hydrogenation leads to a series of H_xNOH_y intermediates, which are finally converted into NH_3 (He et al. 2022a, b). Protonation of H_xNOH_y intermediates requires less energy compared to N* hydrogenation in the dissociative mechanism. Hence, the associative mechanism is thermodynamically more favorable than the dissociative mechanism owing to the absence of N–O bond breakage and the low energy barrier involved in the protonation (Long et al. 2021).

Based on these broad mechanisms, NO reduction pathways can be classified into associative-Tafel, association-Heyrovsky, dissociation-Tafel, and dissociation-Heyrovsky mechanisms (Long et al. 2020). In addition, the hydrogenation step in the associative-Tafel and the association-Heyrovsky mechanism is further classified into specific pathways, named distal or alternative association, as illustrated in Fig. 1. In the distal-oxygen or distal-nitrogen pathway, the oxygen or nitrogen atom in NO is completely hydrogenated to H_2O or NH_3. In the alternating-oxygen or nitrogen pathway, the oxygen or nitrogen atom is first hydrogenated, followed by the hydrogenation of the alternative atom (Fan et al. 2023).

Clayborne et al. (2015) investigated the NO reduction reaction mechanism on Pt (111) using a combination of electrokinetic rate theories and first-principle calculations. The selective reduction of NO occurs along two pathways: the reductive stripping method in a low potential range and continuous NO reduction at a high potential range, producing
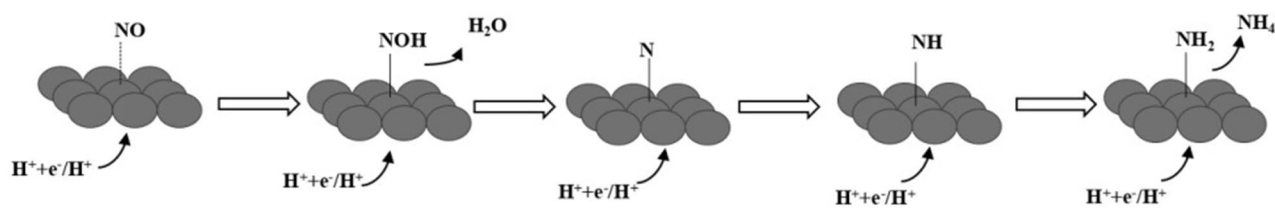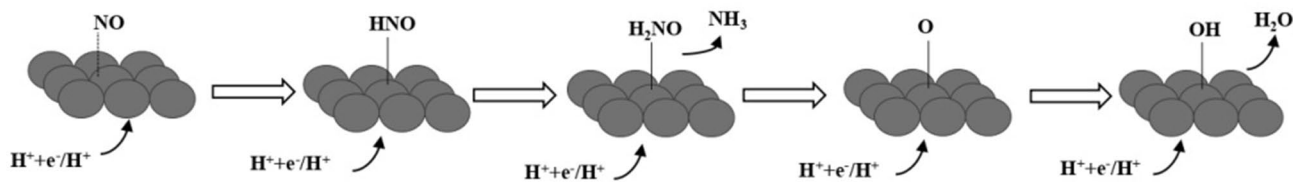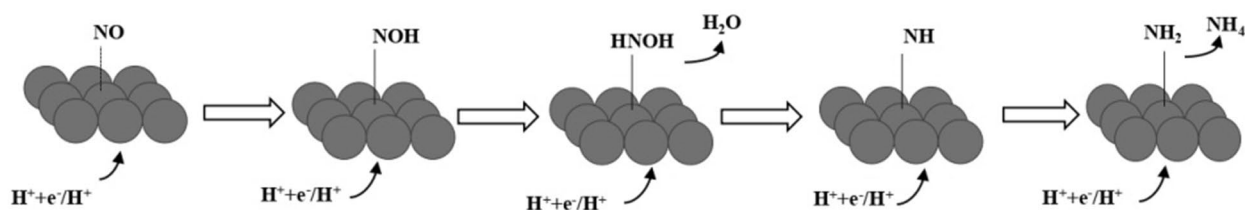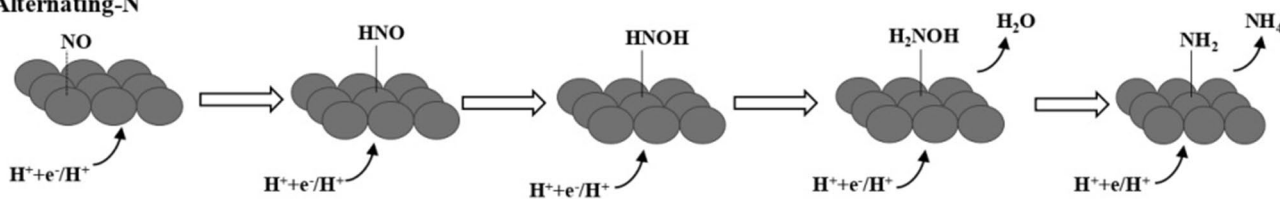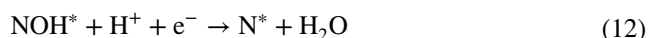

Fig. 1 Different types of associative mechanisms for the conversion of NO to NH_3 in the NO reduction reaction. The associative mechanisms involve distal-oxygen, distal-nitrogen, alternating-oxygen, and alternating-nitrogen pathways. The detailed elementary steps involved in these associative mechanisms with the subsequent protonation of H_xNOH_y intermediates to produce the major product NH_3 and H_2O. The pathway selection is determined by the favorable thermodynamic potential and orientation of the absorbed reactants. Reproduced with permission of the Royal Society of Chemistry from Fan et al. (2023)

NH$_3$ and N$_2$O, respectively. The proposed mechanism for ammonia formation involves two major intermediates: HNO and H$_2$NO. These intermediates were selected based on their lower energy profile compared to NOH and HNOH species (Rosca et al. 2009). Although two regulated pathways exist for the intermediates, both mechanisms involve the activation of the N–O bond via an electrochemical process. In contrast, N$_2$O formation could occur through a Langmuir–Hinshelwood mechanism involving dimers such as ON–NO, NOH–NO, and HON–NOH or an Eley–Rideal mechanism facilitated by solvated NO molecules.

The surface of the catalyst plays a crucial role in the NO reduction reaction by strongly influencing the breaking of the N–O bond, which is the rate-determining step. Through periodic density functional theory calculations, researchers have investigated the reaction pathway and made important observations. At low coverage of NO on Pt (111), the adsorbed NO (NO*) is protonated, forming NOH* (Eqs. 10, 11). Subsequently, NOH* undergoes two simultaneous steps of N–O bond dissociation and O–H formation, producing nitrogen-adsorbed atoms (N*) (Eq. 12). Finally, the subsequent protonation of N* results in NH$_3$ formation (Eq. 13). In contrast, at high NO coverage, studies using a NO-saturated solution have revealed that NO dissociation is less favorable owing to the limited availability of vacant active sites (de Vooys et al. 2001; Liu et al. 2021). In addition, strong lateral interaction leads to the formation of the most stable intermediate, trans-(NO)$_2$ dimer. This dimer, upon protonation, forms the ON–NOH* intermediate, which finally forms N$_2$O (Clayborne et al. 2015).

$$^* + NO(g) \rightarrow NO^* \tag{10}$$

$$NO^* + H^+ + e^- \rightarrow NOH^* \tag{11}$$

$$NOH^* + H^+ + e^- \rightarrow N^* + H_2O \tag{12}$$

$$N^* + 3H^+ + 3e^- \rightarrow{}^* NH_3 \tag{13}$$

Cu (111) is another highly active catalyst for the NO reduction reaction, exhibiting a preference for NH$_3$ formation over hydrogen evolution reaction at a potential near -0.65 V versus Reversible Hydrogen Electrode. Long et al. (2020) conducted density functional theory calculations to investigate the NO reduction reaction mechanism on Cu (111) and found that it follows an association-Heyrovsky mechanism with the distal-oxygen pathway. In this mechanism, the hydrogenation of intermediate NOH* was the most energy-demanding step.

Unlike on Pt (111), where the rate-determining step is the formation of the trans-NO$_2$ dimer, on Cu (111), the protonation of ON–NOH* to form N$_2$O becomes the rate-determining step. At lower potential values, the protonation of N*, occurs with a low energy barrier, facilitating easier continuous hydrogenation compared to N–NO or N–N bond formation required for N$_2$O or N$_2$ formation, respectively. Cu (111) is more active than Pt (111) owing to the absence of competitive hydrogen evolution reaction at lower potentials, as depicted in Fig. 2. In addition, based on kinetic theory calculations, NH$_3$ product formation is thermodynamically more favorable than the production of H$_2$, N$_2$O, and N$_2$ (Fu et al. 2022). Therefore, the high selectivity of catalysts for the selective reduction of NO to NH$_3$ is a crucial parameter in catalyst design.

Zhou et al. (2022) fabricated a metal-free catalyst of two-dimensional hexagonal boron nitride–graphene for enhanced NO reduction. The authors described the catalytic activity for NO reduction by analyzing the energy barrier of the potential-determining step against the overpotential of the electrochemical steps involved. The two possible mechanisms proposed for the NO reduction reaction are illustrated in Fig. 3. These mechanisms are based on the acceptor–donor effect, where the proton–electron attack can occur on nitrogen atoms (nitrogen-side pathway) or oxygen atoms (oxygen-side pathway), depending on their respective affinity for proton–electron pair. In the oxygen-side pathway, hydrogenation occurs on the terminal oxygen atom, producing water and hydrogenation on nitrogen to produce NH$_3$. The reverse occurs in the nitrogen-side pathway. Owing to unstable H$_2$NO and H$_2$NOH intermediates, the subsequent hydrogenation steps face an enhanced energy barrier. It was revealed that the nitrogen-side pathway exhibited thermodynamic favorability over the oxygen-side pathway for converting NO reduction to NH$_3$ on hexagonal boron nitride–graphene heterostructures.

Ko et al. (2022) evaluated the effect of NO partial pressure and pH on the NO reduction reaction. The authors concluded that the concentration of NO coverage led to product selectivity. Specifically, high NO coverage facilitated N–N bonded products such as N$_2$ and N$_2$O, while low NO coverage favored NH$_3$ formation. This observation suggests that the availability of nitrogen sources, including adsorbed NO* or N* and NO in the solution, influences N–N bond coupling. By controlling NO availability, it is possible to enhance the selectivity of desired products of the NO reduction reaction. Wan et al. (2021) conducted a computational mechanistic investigation on various transition metals by examining the limiting potential toward NO reduction reaction. The limiting potential, which is directly correlated with the adsorption-free energy change, represents the negative of the free energy change of proton–electron steps. The results were presented in a volcano plot, which depicted the relationship between the limiting potential (voltage versus

Fig. 2 Comparative illustration of NO reduction reaction occurring on Pt (111) and Cu (111) surfaces. NO reduction reaction on Pt (111) and Cu (111) by analyzing the dependence of surface coverage concentration of reactant molecules and potential variation. It is evident that at lower potentials, Cu (111) is more selective toward NO reduction reaction while suppressing the adsorption of H* compared to Pt (111). The comparative study of Pt (111) and Cu (111) explains the significance of selective adsorption of desired reactants as a crucial parameter in catalyst design for the selective reduction of NO to NH$_3$ as the targeted product
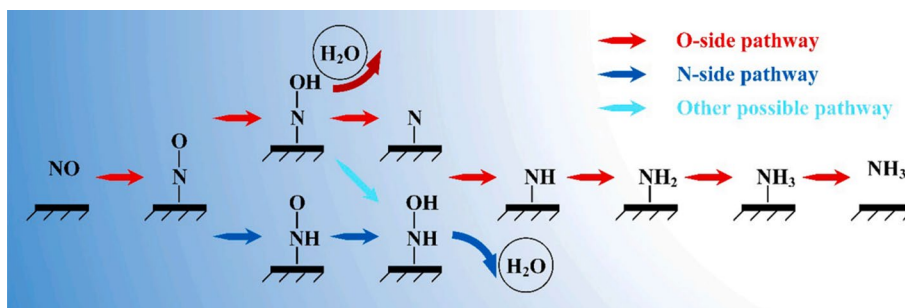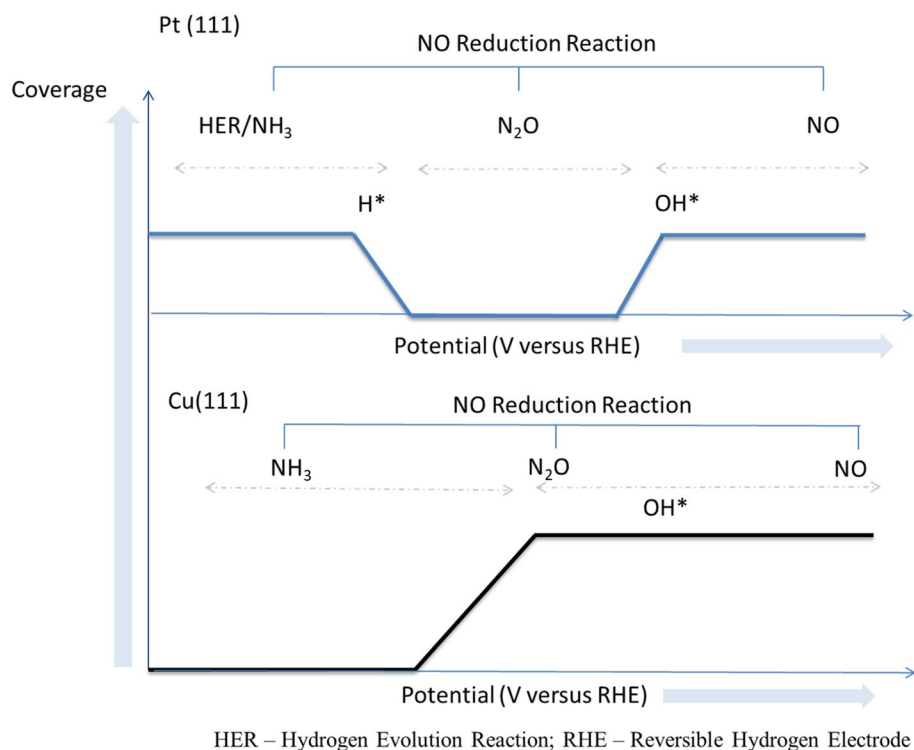
Fig. 3 Two reaction pathways for converting NO to NH$_3$ on hexagonal boron nitride–graphene heterostructures. The NO reduction reaction involves the oxygen- and nitrogen-side pathways. In the oxygen-side pathway, the proton–electron pair attacks oxygen, while in the nitrogen-side pathway, the attack occurs on nitrogen. Subsequent protonation of NO* involves the oxygen- and nitrogen-side pathway, forming NHO* and NOH* intermediates, respectively, to ultimately produce NH$_3$ as a targeted selective product. Reproduced with permission of the Elsevier from Zhou et al. (2022)

reversible hydrogen electrode) and adsorption-free energy change. The plot showed that the hydrogen evolution reaction was favored over the NO reduction reaction for limiting potential below -1.5 eV. Additionally, NO* adsorption became less feasible above -0.83 eV. Cu (111) exhibited the optimum adsorption-free energy change within this range of limiting potentials, making it the most suitable electrocatalyst for selective NH$_3$ formation.

Hydrogen evolution reaction suppression of nitric oxide reduction

To be an ideal electrocatalyst for NO reduction reaction, a material must exhibit maximum Faradaic efficiency at lower over potential. However, this presents a challenge as there is a competing hydrogen evolution reaction occurs at a

similar potential range (Naik Shreyanka et al. 2022; Theerthagiri et al. 2020, 2021). For example, Cu (111) has more selectivity for NH$_3$ formation compared to Pt (111), which is attributed to Pt-based electrocatalysts being well-known electrocatalysts for their proficiency in hydrogen evolution reaction. The active sites of these electrocatalysts compete with the adsorption of NO* and H*. However, slow hydrogen evolution reaction kinetics can limit the availability of the proton source required for the subsequent hydrogenation processes in the NO reduction reaction. Therefore, the catalyst must operate just above the hydrogen evolution reaction overpotential to achieve maximum Faradaic efficiency for the NH$_3$ formation (Carro et al. 2022; de Vooys et al. 2001).

The adsorption energy of NO* is chosen as another descriptor for governing the selectivity of product formation in the NO reduction reaction, in conjunction with the thermodynamics involved in the electrochemical proton–electron coupled intermediate steps (Wan et al. 2021). Figure 4 describes the adsorption energy plot of NO* versus H* for various transition metals. The horizontal line represents the equilibrium between the concentration of NO(g) and adsorbed NO*, while the vertical line represents the equilibrium between ½ H$_2$ and H*. Metals above the horizontal line
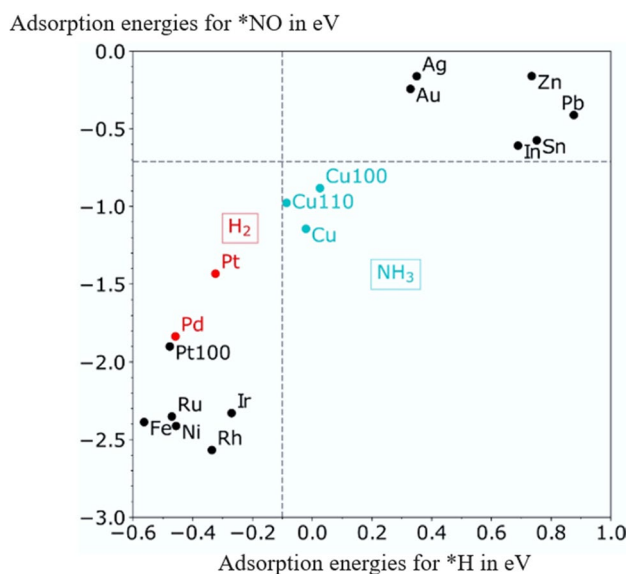

Fig. 4 The adsorption energies of different transition metals. The plot illustrates the adsorption energy of *NO versus H* for various transition metals. The horizontal line represents the equilibrium between the concentration of NO(g) and adsorbed *NO, while the vertical line represents the equilibrium between ½ H$_2$ and H*. Metals above the horizontal line, exhibiting greater adsorption energy of *NO, demonstrate low activity in the NO reduction reaction owing to the unfavorable *NO adsorption energy. Metals to the left side of the vertical line exhibit strong adsorption of *NO and H*, indicating the occurrence of the hydrogen evolution reaction at negative potential values. Metals below the horizontal line show good binding capacity toward *NO adsorption. Reproduced with permission of the Wiley–VCH from Wan et al. (2021)

with greater ΔE_{NO*} exhibit low activity for the NO reduction reaction owing to unfavorable NO* adsorption energy. However, even on these metals with weak binding energy, sufficient NO reduction reaction is observed at complete NO coverage or with saturated NO solutions (Ko et al. 2022). Metals to the left side of the vertical line exhibit strong adsorption of NO* and H*, indicating that the hydrogen evolution reaction occurs at negative potential values. Metals below the horizontal line have a good binding capacity for NO* adsorption. In the case of noble metals, although the binding energy of NO* is thermodynamically feasible, the rapid rate of H* adsorption and hydrogen evolution reaction kinetics results in competitive hydrogen evolution reactions rather than NO reduction reactions. Therefore, metals below the horizontal line have an affinity for NO* and H*, raising the possibility of a competitive hydrogen evolution reaction. However, the Faradaic efficiency of NH$_3$ can be sufficiently enhanced by performing the reaction just above the overpotential of the hydrogen evolution reaction.

Research devoted to selective NO reduction reaction to NH$_3$ conversion has been ongoing for several decades. However, the relationship between reduction steps and electrolyte media has not been well understood. Carro et al. (2022) analyzed the effect of electrolytes on the NO reduction reaction and found that acidic conditions promote competitive hydrogen evolution reactions owing to readily available H$^+$ ions. Better selectivity for the NO reduction reaction was achieved in alkaline and neutral media. In addition, fabricating catalysts with controlled dimensions and morphologies, along with a greater binding energy for NO compared to H*, can effectively enhance NO reduction reaction selectivity.

Theoretical and experimental studies conducted by Long et al. (2021) evaluated the potential dependence of the NO reduction reaction and its competition with the hydrogen evolution reaction through potential-dependent energy barrier calculations and microkinetic stimulations. In the low potential range, the theoretical production rates for both NH$_3$ and H$_2$ showed a linear relationship with the potential. The experimental studies also validated this trend, although a slight decrease in current density for NH$_3$ was observed. This decrease may be attributed to the restricted mass transport of NO at low potentials, which was not included in the theoretical model. At negative potentials, the Volmer step exhibited a favorable step than the protonation of the intermediate step in the conversion of NO reduction to NH$_3$. This explains the increased rates of hydrogen evolution reaction compared to the NO reduction reaction as potential decreases below 0 V versus reversible hydrogen electrode. Present research efforts are therefore focused on conducting NO reduction reactions with suppressed hydrogen evolution reactions by employing nonaqueous electrolytes, such as solid electrolytes

(Chen et al. 2023b; Kwon et al. 2021; Sethuram Markandaraj et al. 2022).

Heterogeneous electrocatalysts for NO reduction reaction

Metal-based catalysts

The electrochemical reduction of NO into NH_3 comprises huge potential in environmental remediation by converting industrial gaseous waste into value-added products and contributing to balance the global nitrogen cycle. Recently, the research on NO electrochemical reduction has primarily focused on metal-based catalysts, both precious and nonprecious. However, the main drawback of these catalysts is the formation of metal–hydrogen bonds, which often leads to the undesired competitive hydrogen evolution reaction and hinders selective NO reduction, as discussed in the previous "Hydrogen evolution reaction suppression on nitric oxide reduction" Section. This drawback was addressed by optimizing the rational design in various electrocatalysts, ensuring high electrocatalytic activity, tunable electronic structure, and robust stability.

Wang et al. (2023) explored a series of single metal atoms (TM=V, Cr, Mn, Fe, Co, Ni, Cu, Ru, Rh, and Ta) anchored on pyrrole-type defective graphene (TM-N_4) catalysts for the electrosynthesis of NH_3 via NO reduction. Among them, Fe–N_4 shows excellent electrocatalytic activity toward NO elimination and NH_3 production with high yield, attributed to the ability of Fe–N_4 to sufficiently adsorb and activate NO molecules. Density functional theory was employed to describe the intrinsic behavior between metal atoms and the N* intermediate in the adsorption-free energy, which established the guidelines for the rational design of effective electrocatalysts toward NO-to-NH_3 generation. Li et al. (2023) investigated hexagonal boron nitride nanoribbons as effective metal-free electrocatalysts for NO electroreduction into NH_3 generation. These nanoribbons demonstrated sufficient chemisorption of NO molecules, particularly over zigzag and armchair configurations, resulting in highly selective NH_3 production without side products, such as N_2, N_2O, and H_2. The enhanced electroreduction of NO was explained by the effective electronic interaction among NO molecules, armchair hexagonal boron nitride nanoribbons, and numerous active sites.

He et al. (2022a) investigated the conducted a theoretical study on designing an S-vacancy FeS_2 catalyst for electrochemical NO reduction reaction and revealed that S-vacancy enhanced the NO reduction into NH_3 under ambient conditions. The processes were found to be exothermic once the O atom of the NO molecule was inserted into the S vacancy and adsorbed side-on. Sethuram Markandaraj et al. (2022) synthesized a core@shell electrocatalyst composed of nickel@nitrogen-doped porous carbon through a two-step process. Initially, a Prussian blue analog was prepared, followed by annealing under an N_2 atmosphere at temperatures ranging from 600 to 800 °C for 3 h. The resulting core@shell structure consisted of a nitrogen-doped porous carbon shell that played a crucial role in preventing the dissolution of Ni nanoparticles, thereby ensuring long-term electrochemical stability during the reduction of NO to NH_3. The optimized nickel@nitrogen-doped porous carbon electrocatalyst exhibited a Faradaic efficiency of 72.3% at 0.16 V versus reversible hydrogen electrode during the NH_3 synthesis electrolysis process. Furthermore, the authors fabricated an electrolyzer with cathodic NO reduction and anodic oxygen evolution reactions using nickel@nitrogen-doped porous carbon as the cathode material and RuO_2 as the anode material, as shown in Fig. 5.

Werchmeister and Hansen (2013) synthesized praseodymium-doped cerium oxide through a combustion route and fabricated a cone-shaped electrode for NO reduction. They studied the different compositions of $Ce_{1-x}Pr_xO_{2-\delta}$ where $x=0.1$–0.4. The NO reduction current increased with increasing Pr content, and the samples $Ce_{0.9}Pr_{0.1}O_{2-\delta}$ and $Ce_{0.8}Pr_{0.2}O_{2-\delta}$ exhibited excellent reduction currents, indicating high efficiency in NO reduction. This performance improvement could be attributed to the improved electronic conductivity resulting from introducing Pr content. Soto-Hernández et al. (2019) fabricated the Pd- and PdCu-supported Vulcan carbon as electrodes via the impregnation method for No reduction. Interestingly, introducing Cu into Pd enhanced the reduction process, leading to excellent electroreduction activity of NO in an alkaline solution. Differential electrochemical mass spectroscopy revealed the generation of N_2, NH_3^-, and N_2H_4 at more negative potentials. Saeidi and Esrafili (2023) investigated C_3N nanosheet electrodes for the electrochemical NO reduction into NH_3 by tuning the surface of C_3N through B doping. The B–C_3N nanosheets exhibited outstanding performance in NO reduction to NH_3 generation at low coverages while N_2 generation at high coverages. Thus, the B atom served as highly reactive sites for NO adsorption, resulting in enhanced NO reduction into NH_3 via *HNO as the main intermediate product.

Liang et al. (2022a) have constructed surfactant-free hydrothermal-assisted iron-oxide nanorods and studied their application in the direct electrochemical conversion of NO into NH_3. The proposed catalyst exhibits outstanding performance in NO reduction under neutral media, achieving a maximum NH_3 yield of 78.02 mol h^{-1} cm^{-2} and a Faradaic efficiency of 1.18 mW cm^{-2}. Theoretical analysis proves the binding of NO over the (104) plane of the Fe_2O_3 catalyst surface through the charge acceptance–donation mechanism.
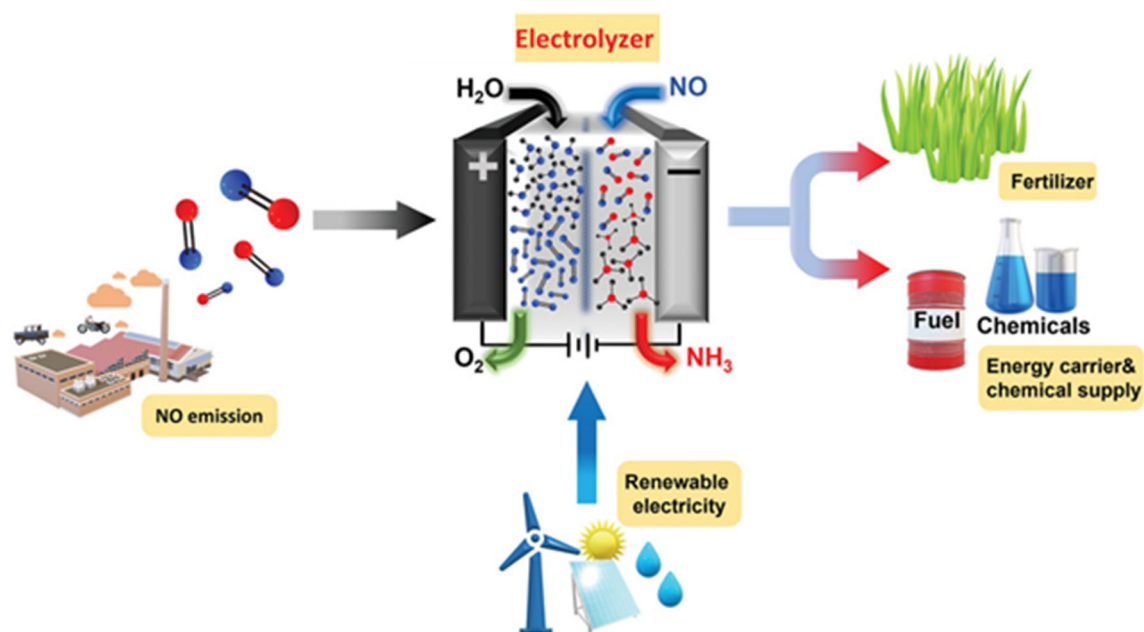
Fig. 5 The strategies involved during electrochemical conversion of NO into NH_3 using an electrolyzer fabricated with cathodic NO reduction and anodic oxygen evolution reactions. The cathode material consisted of nickel@nitrogen-doped porous carbon, while the anode material is RuO_2. The fabricated electrolyzer was powered by renewable electricity. This setup enables the electrochemical conver-sion of NO emissions from fossil fuel combustion in power plants, industries, and automobiles into NH_3, a value-added product. The produced NH_3 can be utilized as fertilizers, fuels, chemicals, and energy carriers. Reproduced with permission of the Wiley–VCH from Sethuram Markandaraj et al. (2022)

Meanwhile, Vooys et al. (2001) developed a series of noble metal electrodes, including Au, Pr, Ir, Rh, and Ru, to efficiently convert NO to NH_3. Interestingly, all tested metals exhibited maximum selectivity toward NH_3 at low potentials and high selectivity toward N_2O at high potentials, and the formation of N_2 occurred at intermediate potentials. Furthermore, the catalytic behavior of transition metals closely resembles that of conventional Pt electrocatalysts, indicating a similar reaction mechanism. Electrochemical analysis indicates a combined electron–proton transfer and non-electrochemical rate-determining step in NH_3 formation.

Ren et al. (2022) explored the potential of a Cu_2Si monolayer electrocatalyst for efficient NH_3 production through NO reduction. Using first-principle calculations, they also systematically investigated the role of incorporating p-block elements into transition metal-based electrocatalysts. Upon comparing the NO reduction performance of pure Cu and Si-doped Cu surfaces, Si atoms reduced the adsorption strength of NO and felicitated the protonation of *NO by reducing the thermodynamic energy barrier. This investigation concluded that introducing f-block elements can modulate surface chemistry and physiochemical properties, enhancing electrocatalytic activity. Zhang et al. (2023) synthesized boron phosphide via a vacuum-sealing approach, as a metal-free electrocatalyst for NO removal and NH_3 production. Boron phosphide exhibited weak H-binding, which can hinder the competing hydrogen evolution reaction. After the adsorption of NO molecules over boron phosphide, *NO spontaneously formed bonds with boron and phosphorous atoms through side-on adsorption, leading to electron transfer from boron and phosphorus atoms to *NO molecules. This created an electron-rich area around *NO and a deficient area around boron and phosphorus atoms, enabling efficient NO activation through the synergistic effect of boron and phosphorus. Long et al. (2020) explored Cu foam as an electrode for NO reduction to NH_3, achieving a yield rate of 517.1 μmol cm^{-2} h^{-1} and a Faradaic efficiency of 93.5% at -0.9 V versus reversible hydrogen electrode. Their investigation highlighted that Cu-based materials are the most effective catalysts among the other transition metal-based catalysts in selectively producing NH_3 while minimizing the other byproducts, such as N_2, H_2, and N_2O.

Carbon-supported catalysts

Carbonaceous materials are highly valued owing to their physiochemical properties, including large porosity, good conductivity, and outstanding surface chemistry (Lee et al. 2021; Li et al. 2021; Mokhtar et al. 2022; Muradov et al. 2005; Yu et al. 2022). Henceforth, they have been vastly employed as potential catalyst supports in heterogeneous catalytic processes. Carbon-based materials have become

a growing interest in the research community as renowned catalyst materials (Auer et al. 1998). Widely used carbon supports for catalyst preparation include activated carbon, carbon black, reduced graphene oxide, carbon nanotubes, graphitic carbonitride, and graphene (Auer et al. 1998; Xia et al. 2022). The implementation of carbonaceous materials as catalyst supports offers several advantages. Their high surface area and porosity enable efficient dispersion of the active phase. The pore size of the supports could be changed to meet the necessities of specific catalytic reactions. The surface chemistry of carbonaceous supports plays a predominant role in determining the overall catalytic performance, specifically during the synthesis process. Carbonaceous materials usually exhibit hydrophobic nature, showing minimal affinity toward polar solvents such as ethanol, methanol, and water, while demonstrating a stronger affinity for nonpolar solvents like chloroform, acetone, and dichloromethane. However, the surface chemistry of carbon supports can be easily modified when they interact with the active components of the catalysts, thereby leading to a uniform distribution of active material over the carbon supports. Besides the facile alteration of surface chemistry and porous structure, carbonaceous supports possess various beneficial characteristics (Rodríguez-reinoso 1998; Stüber et al. 2005): (a) they are mostly inexpensive compared to other conventional catalysts supports such as alumina and silica, (b) their porous structure allows for the production of catalysts in various shapes such as powder, pellets, films, fibers, and granules, (c) the substantial composition of carbon enables catalysts to function and remain stable even at high temperatures (> 800 °C), (d) metals can be easily reduced over carbon supports, and (e) they exhibit high retardance toward various acids and bases. Recently, numerous industries have utilized carbon compounds as the support materials for catalysts. The prepared carbon-supported catalyst is used for many organic reactions, including oxidation, halogenation, desulphurization, and nitrogenation. Contrarily, many industrial processes release harmful gases during synthesis, creating an unfavorable and hazardous atmosphere (Stüber et al. 2005).

NO_x, consisting of NO_2 and NO, is recognized as a significant industrial gaseous contaminant and major pollutants, resulting from the combustion of fossil fuels, with an estimated global emission of 5.35×10^7 T. Currently, the scientific community has shown great interest in the removal of nitric oxide, especially from industrial exhausted gas, and the NO reduction into NH_3. In this regard, various approaches have focused on introducing different metal species over the carbon support surface. However, the inert and hydrophobic nature of carbon supports necessitates a pre-treatment functionalization process to integrate them with metal or metal oxides. Regrettably, current preparative processes suffer numerous experimental challenges, including catalyst particle agglomeration, unusual deposition, and

undesirable large-sized particles. For instance, introducing metal oxide functional groups over the carbon nanotubes often compromises the unique properties of carbon allotropes, resulting in low catalytic performance (Anthonysamy et al. 2018). Henceforth, more synthetic protocol with less damage to carbon nanotube properties needs to be progressed, which is vital to decontaminate bare carbon nanotubes from impurities such as amorphous carbon, coal, fullerenes, and catalyst particles during production. One powerful method for functionalizing, purifying, and activating carbon nanotubes is a wet-chemical strategy, where they are dissolved in appropriate oxidizing agents for a specified duration, sometimes aided by heat to accelerate the oxidation process. Acid treatment is widely employed for surface oxidation of most carbon supports using nitric acid, sulfuric acid, or a combination of both. This acid treatment process facilitates the formation of functional groups such as –C=O, –COOH, and –OH over the carbon nanotube surface (Zhao et al. 2022), with the extent of oxygen-containing groups depending on the specific treatment method employed. Functionalizing the surface of a multiwalled carbon nanotube is essential for attaching metal nanoparticles over the oxygenated carbon support. Acid treatment enables the covalent addition of oxygenated groups over the surface and open ends of carbon nanotubes, improving the dispersion of the chosen metal species over the carbon support. Numerous preparative methods, including sol–gel, impregnation, incipient wetness, and pyridine thermal treatment, could improve the overall dispersion of metal species over the carbon support surface. Henceforth, developing a valid fabrication process for carbon-related catalysts is crucial for achieving excellent catalytic performance (Zhao et al. 2019).

Pure carbon-based support and templates

In the early 90 s, Teng et al. (1992) studied NO reduction using carbon materials through thermogravimetric analysis. To investigate the process, they employed two different thermogravimetric methods, namely transient reaction and pseudo-steady methods. Their findings revealed that N_2, CO_2, and CO resulted from the NO reduction. However, during that time, the electrocatalytic synthesis of NH_3 from NO was not progressed. In the later years, the direct synthesis of NH_3 from the NO reduction reaction is gradually explored, but limited reports have been available to date on carbon-based catalysts and carbon support for the efficient catalytic activity in the NO reduction reaction. In the following sections, we provide some notable examples of these studies.

Ouyang et al. (2022) reported the synthesis of a highly active metal-free catalyst for efficient NO reduction to NH_3, consisting of honeycomb carbon nanofiber coated over the surface of carbon paper. The honeycomb carbon nanofibers were initially prepared for an electrospinning process,
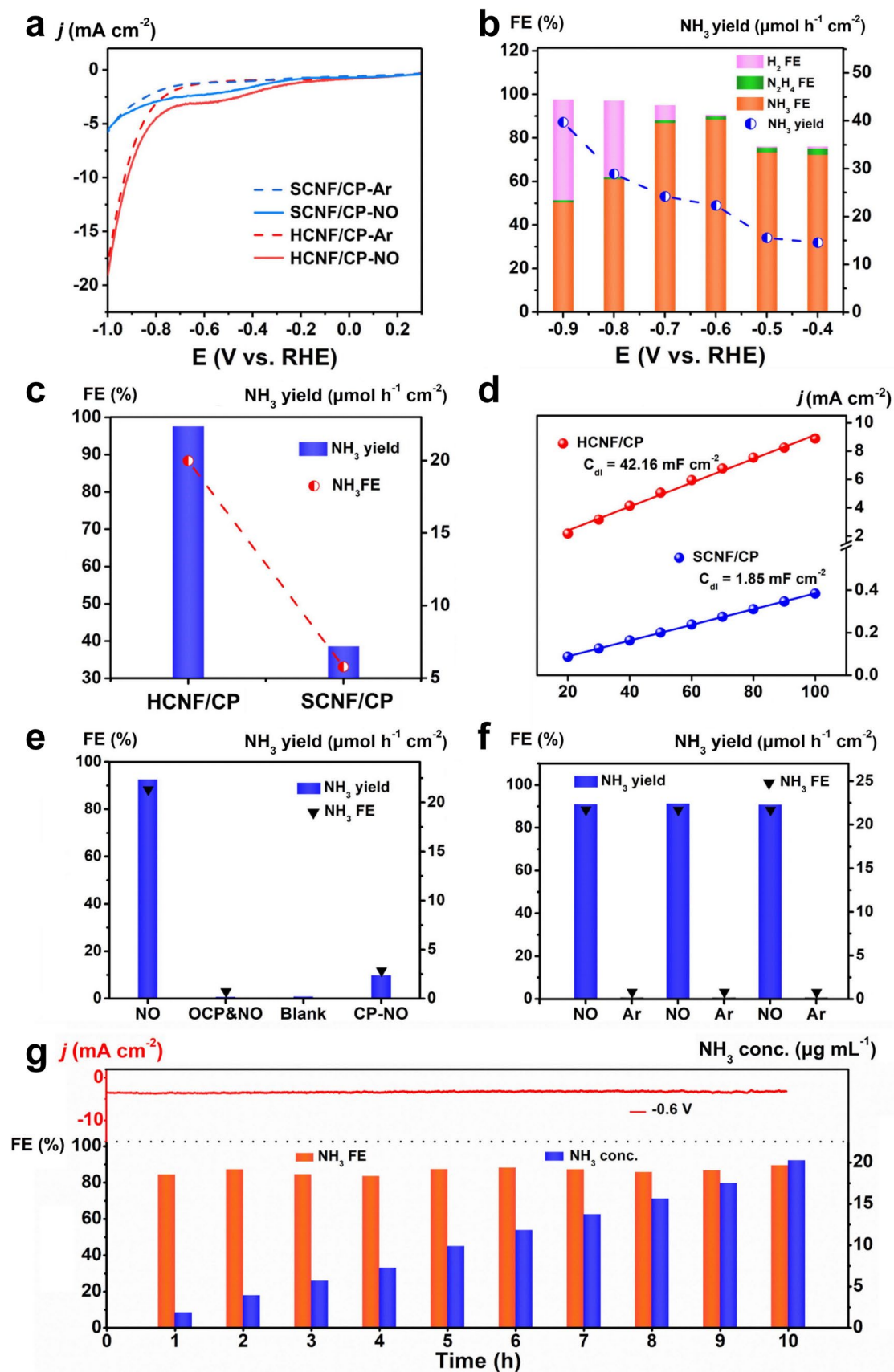
followed by calcination at 800 °C, forming the desired catalyst. For comparison, solid carbon nanofibers were also prepared. The catalytic reduction reaction was performed in an electrolyte of 0.2 M Na_2SO_4 under a mixed gas atmosphere of a 1:3 ratio of NO:Ar. The catalytic activity of the honeycomb carbon nanofiber on carbon paper catalyst was evaluated, as shown in Fig. 6a, revealing a wide potential range of −0.3 to −0.8 V compared to its pristine counterpart, confirming its excellent catalytic activity. In addition, the catalyst displayed inferior NO reduction in 0.1 M NaOH and 0.1 M HCl solutions, as depicted in Fig. 6b. Figure 6b also represents the superior catalytic activity of the as-constructed solid carbon nanofiber on carbon paper and honeycomb carbon nanofiber on carbon paper catalyst for NH$_3$ synthesis, achieving the highest NH$_3$ yield of 22.5 µmol h^{-1} cm^{-2} with an outstanding Faradaic efficiency of 88.3%. The optimized limiting potential was −0.6 V. Compared to the solid carbon nanofiber on carbon paper, the honeycomb carbon nanofiber on carbon paper catalyst showed improved Faradaic efficiency, as shown in Fig. 6c, while the solid carbon nanofiber on carbon paper catalyst yielded NH$_3$ with a low yield of 7.1 µmol h^{-1} cm^{-2} and a Faradaic efficiency of ∼33.09%. The high catalytic activity of honeycomb carbon nanofiber on carbon paper in the NO reduction reaction might be attributed to its high electrochemically active surface area and the exposure of additional active sites, as shown in Fig. 6d. In addition, the interconnected nanocavities of the catalyst could easily trap NO gas to improve the interaction between the catalyst and NO moieties, thereby yielding enhanced efficacious NO reduction. Control experiments were performed to verify the NH$_3$ formed by the electrocatalytic NO reduction reaction method using the as-prepared catalyst. As depicted in Fig. 6e, a negligible yield of NH$_3$ was obtained at the open

circuit potential for the post-electrolysis electrolyte, ruling out contamination from the electrolyte and experimental setups. The catalyst performance was assessed over six cycles for 1 h in both NO- and Ar-saturated environments for the prepared catalysts, as shown in Fig. 6f, with results indicating improved conversion of NO to NH$_3$ by the honeycomb carbon nanofiber on carbon paper catalyst. Figure 6g displays the durability of the catalyst at −0.6 V during continuous electrolysis of 10 h, demonstrating that the catalyst remains structurally stable and retains its morphological features even after durability measurement.

Nonmetallic compound-incorporated carbon support catalysts

Owing to their excellent catalytic behavior, noble metal-incorporated carbon support catalysts have been extensively studied for the NO reduction reaction. The presence of carbon support aids in maintaining robust active sites even under large loads of noble metals, thereby improving the catalytic divergence and active surface area. This phenomenon improves the overall utilization of the materials during catalytic activity.

In early 2019, Soto-Hernández et al. (2019) prepared a series of noble metal-based Pd and PdCu catalysts supported over carbon Vulcan through a facile impregnation route. Under alkaline conditions, these catalysts were studied as potential catalysts for various catalytic reduction reactions, such as NO_3^-, NO_2^- and NO and NO_2. The prepared carbon-supported Pd and PdCu NPs possessed an average particle size of 12 and 3 nm, respectively. The Cu inclusion into the noble metal matrix improved the overall catalytic reduction, showing the best electroreduction performance for all NO_3^-, NO_2^-, NO, and NO_2 solutions. Electrochemical mass spectrometry confirmed the formation of the various products, such as N_2, NH$_3$, and N_2H_4, from their respective solutions. In addition, the reduction of Faradaic current was approximately six times higher in the saturated NO and NO_2 solutions.

Although Pt- or Pd-based catalysts have shown excellent performance toward electrochemical NO reduction reactions, their high cost, elevated reaction temperature, and poor long-term stability restrict their commercial viability. Henceforth, substituting these noble metal catalysts with inexpensive, earth-abundant, high-efficiency catalysts are largely desirable. Addressing this purpose, Saeidi et al. (2021) demonstrated Si-incorporated N-doped graphene to improve NO reduction performance to NH$_3$ through theoretical models. Based on calculated adsorption energy, they inferred that a single Si-atom doping into the N_4G vacant sites produces a Si–N_4G catalyst for NO reduction to NH$_3$. Their study also concluded that electrochemical NO reduction produces NH$_3$ at low coverages and N_2 at high coverages, with the

NO moiety being reduced at a limiting potential of 0.56 eV under ambient conditions. Moreover, the resulting significant molecules, such as NH_3 and N_2, are less carcinogenic than NO molecules, making this work potentially valuable in removing hazardous NO molecules from the environment.

In previous studies, carbon-doped boron nitride was investigated as a potential NO reduction reaction catalyst through the density functional theory mechanistic principle by Mudchimo et al. (2018). In this process, a trans-$(NO)_2$ was identified as the key intermediate in the reaction, which was kinetically and thermodynamically favorable. The observed rate-limiting potential of 0.62 eV indicated that the carbon-doped boron nitride could be a metal-free catalyst for eco-friendly NO reduction under ambient conditions. Based on this concept, Esrafili and Arjomandi Rad (2019) later studied the effect of carbon-doped boron nitride for efficient sensing and detection of NO and NO_2 through theoretical calculations. They observed that the localization of high-spin density localized at the surface C atom was responsible for the strong adsorption energy of NO_2 and NO. The prepared catalyst showed low sensitivity toward molecules such as CO_2, CO, NH_3, and H_2O. Likewise, Zhou et al. (2022) developed a metal-free catalyst by introducing C_{center}–CN_2 into hexagonal boron nitride-graphene materials to enhance the NO reduction reaction for NH_3 synthesis. Through band theory and molecular orbital theory, they studied the mechanism of this catalyst and discovered specific active sites in the form of C_{center}–CN_2 over the hexagonal boron nitride interface. This heterostructured hexagonal boron nitride-graphene catalyst provides an ultralow limiting potential of −0.22 V, suggesting its excellent NO reduction activity. This remarkable catalytic activity might be attributed to the unique structural configuration at the modified interface of hexagonal boron nitride-graphene. In addition, this doping protocol could be employed for developing NO reduction catalysts using other 2D materials, including graphitic carbonitride, graphene, and graphitic boron carbide.

In a subsequent study, Peng et al. (2020) constructed a sequence of single metal catalysts, such as niobium-decorated boron and nitrogen-codoped carbon nanotubes, for efficient electrochemical NH_3 production through NO reduction (Peng et al. 2020). Interestingly, the catalyst was obtained by dissolving the melamine foam in niobium oxalate, boric acid, and polyethylene glycol complex and then annealed at 900 °C. The existence of carbon nanotubes in the catalyst structure not only improved the electrical conductivity with the aid of heteroatoms boron and nitrogen but also provided copious anchoring sites for the single niobium metal atoms. Stable and efficient catalysts to favor the multiple proton-coupled electron transfer processes are essential for the active transformation of NO to NH_3 through electrochemical reduction. Based upon this concept, Liang et al. (2022a, b) developed a three-dimensional catalyst comprising boron carbide anchored over titanium oxide nanobelts, denoted as $B_{2.6}C$–TiO_2–Ti array, and studied its improved activity toward the NO reduction reaction to NH_3 (Liang et al. 2022a, b). The resultant catalyst exhibited lower over potential and higher current density compared to its pristine counterparts, $B_{2.6}C$–Ti and TiO_2–Ti. This led to a high NH_3 generation yield of 3678.6 μg h^{-1} cm^{-2} with an outstanding Faradaic efficiency of 87.6%, surpassing that of $B_{2.6}C$–Ti (~ 2499.2 μg h^{-1} cm^{-2}, 85.6%, respectively) and TiO_2–Ti (~ 563.5 μg h^{-1} cm^{-2} and 42.6%, respectively). More importantly, the composite catalyst showed long-term stability during 12 h of continuous electrolysis and achieved a maximum power density of 1.7 mW cm^{-2}. Their corresponding catalytic mechanism was evaluated through density functional theory analysis, revealing that C–B bonding at the $B_{2.6}C$ layer efficiently inoculated electrons to NO, stimulating NO and facilitating the reduction process with minimal energy inputs.

Introducing a nonmetal phosphorous element into the carbon support controls the coupling between multiple intermediates and transition metal active centers, thereby facilitating the direct transformation of NO to NH_3. Rising from the finite orbitals, the p-orbital atom is usually inert toward the lone pair electrons of NO. Nevertheless, their properties could be engineered through the electronic configurations of the adjacent transition metal active centers, favoring donation–back-donation mechanisms. For instance, Wu et al. (2021b) proposed a single graphene layer doped with p-orbital element as a promising metal-free catalyst for the acute conversion of NO to NH_3 through theoretical modeling. They found that compared to single the p-atom doping, the adsorption of double p-atom-doped graphene single layer was more thermodynamically feasible, consistent with the Bader charge measurement and differential charge density analysis. This observation indicates a greater charge transfer between adsorbed NO and the double p-atom-doped graphene single-layer catalyst compared to single p-atom-doped graphene. Especially, the double p-atom-doped graphene single layer displayed outstanding selectivity and high catalytic activity, attributed to the density of states and sp^3 hybridization of the p-element. Microkinetic modeling measurements revealed the highest turnover frequency of 8.9×10^5 s per site at 400 K for the NO reduction reaction to NH_3, providing an ultrarapid reaction rate. Henceforth, this work represents the first reported metal-free catalyst for NO elimination and offers an efficient and promising platform for NH_3 synthesis. Similarly, the catalytic mechanism of p,s-doped transition metal biatoms supported by graphene monolayer catalysts has been verified through theoretical first-principle calculations (Zang et al. 2023). This work provides a new pathway for the coherent design and development of dual atomic catalysts for the NO reduction reaction.

Owing to the unsatisfactory Faradaic efficiency and activity of the current, Wu and Yu (2023) investigated the potential viability of eight metal dimer-decorated PC_6 monolayers for the superior catalytic reduction of NO to NH_3 under mild experimental conditions through microkinetic modeling and first-principle calculations. Various catalysts, such as Fe_2–PC_6, Mn_2–PC_6, Cr_2–PC_6, and Re_2–PC_6, were investigated, in which the Fe_2–PC_6 showed better catalytic behavior for NO reduction reaction. To reduce the competing hydrogen evolution reaction and enhance the Faradaic efficiency, the NO adsorption strength of catalysts must be higher than that of protons. In this context, they have computed and compared the adsorption Gibbs free energies of protons and NO over the proposed catalysts.

Recently, a series of metal borides termed as MBenes, derived from group IVB and V transition elements such as Fe_2B_2, Mn_2B_2, and Rh_2B_2, which are similar to transition metal carbides and nitrides, have been constructed for their excellent electrocatalytic activity for NO reduction by Xiao et al. (2021). They have studied the plausible catalytic mechanism of the NO reduction reaction through density functional theory modeling and showed some promising outputs. Theoretical modeling revealed high catalytic activity with limiting potentials of -0.17, -0.01, -0.25, -0.16, and -0.11 V for Hf_2B_2, Ta_2B_2, Zr_2B_2, Ti_2B_2, and Nb_2B_2 MBenes, respectively, toward the NO reduction process. This process paves a new way to scrutinize the highly efficacious catalyst for developing the NO reduction reaction.

Transition metal and metal oxide-incorporated carbon support catalysts

Cobalt-incorporated carbon supports Ir, Pd, Pt, and Ru-based noble metals have been extensively studied as electrocatalysts to fasten the reaction kinetics of the NO reduction reaction; however, their limited marketable availability, low abundance, and high cost restrict their widespread application in NO reduction. Currently, various transition metal-based catalysts, including single atoms, transition metals, chalcogenides, phosphides, and oxides, have been developed for NO reduction to NH_3 and NH_2OH. However, attaining a robust electrocatalyst that enables efficient NO-to-NH_3 conversion with low overpotential still vestiges a drawback. To address this challenge, cost-effective cobalt phosphide nanowires grown over carbon cloth were fabricated through a hydrothermal strategy (Xiao and Shen 2021). This catalyst showed excellent catalytic activity toward NO reduction reaction in an alkaline medium at very low overpotentials. This catalyst achieved the highest NH_3 generation rate of 380 μmol h^{-1} cm^{-2}, outstanding Faradaic efficiency of 91.6%, and a low limiting potential of -0.3 V versus reversible hydrogen electrode, respectively. The catalyst demonstrated robust stability and maintained its catalytic

activity over ten continuous repeated electrolysis tests. Furthermore, Wang et al. designed a series of Co–N_4 moieties incorporated into the graphene layer to improve the electroreduction of NO, as analyzed through density functional theory computations (Wang et al. 2018). They observed that the Co–N_4@Graphene catalyst exhibited the formation of NH_3 at low coverage and N_2O formation at high coverages. Compared to well-established Pt-based catalysts, this proposed catalyst system possessed a better onset potential of -0.12 V, indicating its excellent catalytic behavior. The high thermal stability and excellent catalytic activity of Co–N_4@Graphene make it a promising candidate for NO reduction reactions.

A completely new synthetic techno-economic strategy comprised of tandem plasma electrolysis has been proposed later by Wu et al. for the direct electrochemical synthesis of NH_3 from NO using a nitrogen-doped carbon catalyst with a single cobalt atom (Wu et al. 2021a). This plasma electrocatalysis-derived catalyst demonstrated a high NH_3 yield rate of 1.43 mg_{NH3} cm^{-2} h^{-1} and a superior Faradaic efficiency of 100%. The ultralow limiting potential of -0.33 V versus Reversible Hydrogen Electrode was observed, and the catalyst remained stable over 50 h of operation. At -0.63 V, the NH_3 yield reached 1.43 mg_{NH3} cm^{-2} h^{-1} with a Faradaic efficiency of 62%. This effective synthetic protocol challenges the Haber–Bosch production of NH_3 in terms of yield and activity. Similarly, Liu et al. (2021) reported a series of phthalocyanine sheet catalysts doped with single atoms, such as Ru, Mo, Nb, V, Cr, Fe, Mn, Ni, Co, Zn, Mo, and Cu, showing improved activity for NO reduction to NH_3 through density functional theory computations. These alternative catalyst systems were proposed as a cost-effective and efficient alternative to noble metal catalysts. Among the various single-atoms-based phthalocyanine sheet catalysts, the Co-phthalocyanine catalyst exhibits the highest activity for the NO reduction reaction, achieving a low limiting potential value. The study revealed the formation of NH_3 at low coverages and N_2O at high coverages with a low energy input of 0.58 V. This study contributes to the environmental remediation of denitrification and provides an improved yield rate for NH_3 production.

Nickel-incorporated carbon supports Electrocatalysis has emerged as a promising alternative to the industrial Haber–Bosch process for NH_3 synthesis under ambient environments. In this regard, a single-Ni-atom–anchored nitrogen-doped carbon (Ni@nitrogen-doped carbon) nanostructure catalyst was recently explored to reduce NO to NH_3 (Sethuram Markandaraj et al. 2022). Through a series of control experiments, they concluded that the active center responsible for the NO reduction reaction is the Ni atom in the Ni@nitrogen-doped carbon core–shell structure. In addition, the outer layer of the nitrogen-doped carbon pre-
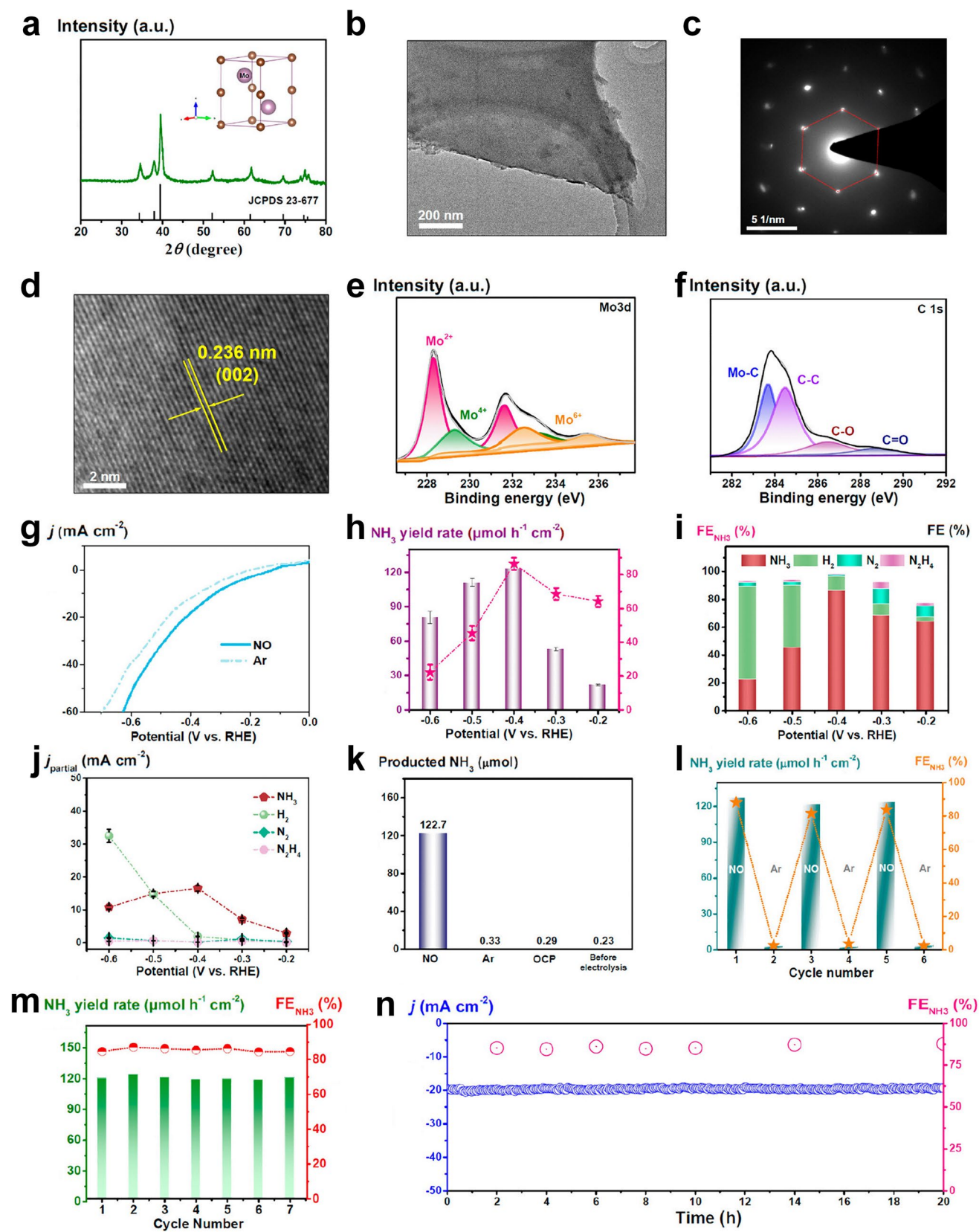
◄**Fig. 7** Structural characterization and electrochemical performance of Mo_2C nanosheets **a** X-ray diffraction pattern of Mo_2C nanosheets which agrees with the standard Joint commission of powder diffraction standard data 23–477, inset of (**a**) represents the crystal structure of Mo_2C. **b–d** High-resolution transmission electron micrographs of Mo_2C nanosheets at different magnifications, including 200, 5, and 2 nm. Ultrahigh-resolution X-ray photoelectron spectroscopy scan of **e** Mo $3d$ in the binding energy range between 225 and 240 eV and **f** C $1s$ in the binding energy range between 292 and 283 eV. **g** Linear sweep voltammetry curve of Mo_2C nanosheets under various conditions, including Ar and NO-saturated electrolyte. **h** Faradaic efficiency and NH_3 yield of Mo_2C nanosheets at various potentials in the range between -0.5 and -0.2 V. **i** Faradaic efficiency plot for different gas products such as N_2, N_2H_4, NH_3, and H_2 at the potential window of -0.2 to -0.5 V. **j** Potential versus partial current density plots for various products such as N_2, N_2H_4, NH_3, and H_2. **k** NH_3 yield under different environments, including open-circuit potential, Ar-feeding gas, and before electrolysis. (**l**) Switching measurement for NO–Ar. **m** Cycling test over Mo_2C nanosheet catalyst for NH_3 production over seven consecutive cycles. **n** Durability analysis over the surface of Mo_2C catalyst for the prolonged duration of 20 h. Reproduced with permission of the American Chemical Society from Chen et al. (2023a). *RHE* Reversible Hydrogen Electrode, *a.u.* arbitrary unit, *vs.* versus, *FE* Faradaic efficiency

vented the Ni de-metalation and corrosion, providing long-term stability during the NO reduction reaction. Henceforth, the proposed Ni@nitrogen-doped carbon catalyst exhibited a high Faradaic efficiency of 72.3 and a low overpotential of 0.16 V, making it a promising candidate for NH_3 synthesis. Moreover, a full-cell electrolyzer was developed by combining RuO_2 as the anode for oxygen evolution reaction and Ni@nitrogen-doped carbon as the cathode for NO reduction, which affords robust performance at 1.5 V even after 20 cycles, with an overall Faradaic efficiency of over 50%. Therefore, this approach provides a promising pathway for robust NH_3 production from NO.

Based on this concept, Meng et al. (2022b) prepared bimetallic NiFe-layered double hydroxide catalysts in the form of nanosheet arrays and nanosheet particles over a carbon foam substrate using ethylene glycol-assisted hydrothermal. These catalysts were effective for NO reduction to NH_3 and an efficient cathode for Zn–NO batteries. The NiFe-layered double hydroxide catalyst demonstrated a maximum Faradaic efficiency of 82% and an NH_3 yield rate of 112 μmol h^{-1} cm^{-2}, demonstrating long-term stability over 30 h with the same NH_3 yield percentage. To further validate the superior activity of the designed catalysts, a Zn-NO battery was constructed, delivering a large NH_3 yield rate of 32 μmol h^{-1} cm^{-2} and an outstanding power density of 1.8 mW cm^{-2}.

Iron-incorporated carbon supports In the biological conversion of nitrite into N_2, N_2O, and NO reductase, heme proteins play a vital role, with one heme group catalyzing the selective bio-reduction of NO into N_2O, followed by the binding of iron center to another heme group. However, the stability of the transition metal complexes is a major challenge owing to the degradation of organic ligands. To avoid such stability issues, Toth and Anson (1989) constructed polyoxotungstates catalysts, where the tungsten cage functions as the base for multiple electrons, facilitating the conversion of NO to NH_3. Especially the catalyst can store and offer electrons to the bound substrate, which is one of the interesting factors in the conversion of NO to NH_3. Kim et al. (2021) fabricated an atomically dispersed iron catalyst for efficient NO reduction to NH_3. However, the resulting product obtained was NH_2OH, exhibiting high selectivity. Despite iron being one of the most abundant metals on earth's crust, the development of iron-based catalyst nanostructures for the durable and active conversion of NO to NH_3 has received little attention until now. Concurrently, the investigation of NO reduction to NH_3 using iron-supported carbon catalysts holds great concern, as it represents a significant step toward evaluating nitric oxide removal electrochemistry and constructing alternative technologies for NH_3 production.

In recent times, Kim et al. (2020) designed a unique silver electrode integrated with an EDTA-Fe^{2+}-based electrolyte to enhance the NO reduction reaction activity and improve the yield rate of NH_3 production. This proposed system showed remarkably low limiting potential -0.165 V versus reversible hydrogen electrode and a current of 50 mA cm^{-2}, producing NH_3 with high selectivity. Furthermore, it exhibited an ultrahigh Faradaic efficiency of 100% over 120 h, confirming the supremacy of the designed catalyst. This strategy opens new ventures for efficient NH_3 production from renewable electricity sources. Very recently, Fe_2O_3 nanorods coated over a carbon paper catalyst were developed to verify its bifunctional activity in the denitrification of NO and NH_3 production through electroreduction by Liang et al. (2022a). Under neutral conditions, the proposed catalyst demonstrated a high Faradaic efficiency of 86.7% and a large NH_3 yield of 78.02 μmol h^{-1} cm^{-2}. Using a similar catalyst as the cathode materials for NO and RuO_2 as the anode, a Zn–NO battery was fabricated, showing excellent catalytic activities, including an NH_3 yield of 145.28 μg h^{-1} mg$_{cat.}$$^{-1}$ and a power density of 1.18 mW cm^{-2}. Density functional theory simulations indicated that the Fe_2O_3 surface binds to NO through robust electrostatic interaction and follows a charge donation–acceptance mechanism mainly stimulated through the $2\pi*$ back-donation effect.

Other transition metal-based carbon catalysts Molybdenum-based compounds are largely attractive owing to their high catalytic behavior to stimulate nitrogenous materials. Molybdenum sulfide (MoS_2) is one of the active catalysts for the NO reduction reaction owing to its active metal edge sites for the N=O cleavage and activation (Zhang et al. 2021). However, the inert basal planes and low electronic

conductivity of MoS_2 restrict its NO reduction reaction activity. Henceforth, recent focus has shifted toward highly conductive molybdenum carbide (Mo_2C)-based catalysts, which fully expose active Mo edge sites. For the first time, Mo_2C nanosheets were prepared through thermal annealing of MoO_3 by Chen et al. (2023a) and studied as a potential catalyst for the electro-conversion of NO to NH_3. As shown in the X-ray diffraction pattern in Fig. 7a, the prepared catalyst existed in β-form, while the corresponding transmission electron micrograph and selected area electron diffraction pattern confirmed the nanosheets structure with an interplanar distance of 0.23 nm for the (002) reflection plane of β-Mo_2C, as displayed in Fig. 7b–d. In the prepared catalyst, the valence states of Mo were 4+ and 6+, as shown in Fig. 7e. Furthermore, the catalyst exhibited the characteristic signal for the Mo–C bond at 283.7 eV, as shown in Fig. 7f, thereby suggesting the formation of Mo_2C nanosheets. The electrochemical catalytic activity of Mo_2C toward the NO reduction reaction was validated in an air-locked H-type cell using a NO-saturated 0.5 M Na_2SO_4 solution. The resulting linear sweep voltammetry curve displayed in Fig. 7g suggested higher current density in the NO-saturated electrolyte compared to the Ar-saturated electrolyte, confirming the existence of NO reduction reaction over the Mo_2C catalyst. Remarkably, the proposed Mo_2C catalyst showed excellent NO reduction reaction activity with the highest Faradaic efficiency of 86.3% and NH_3 yield rate of 122.7 µmol h^{-1} cm^{-2}, as shown in Fig. 7h. Moreover, the formation of side products N_2H_4 and N_2 led to low Faradaic efficiency and current densities, as shown in Fig. 7i, j. A long-term cycling stability test with Ar–NO confirmed a large NH_3 yield for NO-fed gas, whereas Ar-fed gas displayed a low NH_3 yield (Fig. 7k, l). In addition, prolonged cycling tests over ten cycles of continuous electrolysis demonstrated no apparent changes, proving the extended durability of the catalyst, as depicted in Fig. 7m. Over 20 h of continuous electrolysis, only minor decrements in Faradaic efficiency and current density were observed (Fig. 7n), confirming the ability of the catalysts for long-term NO reduction reactions. Very recently, Meng et al. (2022a) developed MoC nanocrystals surrounded by N-doped carbon nanosheets and studied them as a durable NO reduction reaction catalyst for a high yield rate of NH_3. The resultant catalyst exhibited the highest Faradaic efficiency of 89% ± 2% for the NO reduction reaction. Furthermore, the proposed catalyst showed a promising yield generation rate of 1,350 ± 15 µg h^{-1} cm^{-2} within a limited potential of −0.8 V versus reversible hydrogen electrode. Even after 30 h continuous electrolysis in the NO reduction reaction test, the catalyst showed negligible current density with an improved NH_3 generation rate, confirming the high stability of the catalyst. When the same catalyst was tested as a cathode in a Zn–NO battery with RuO_2 anode, it achieved the highest power density of 1.8 mW cm^{-2}, surpassing

previously reported NO reduction reaction catalysts. This study suggests that Mo-based compounds offer tremendous opportunities to discover highly active and stable catalysts for NH_3 generation.

Wu et al. (2019) constructed a cost-effective, single-atom Cu@g-C_3N_4 catalyst consisting of single copper atoms supported on graphitic carbon nitride with high stability and activity for NO electroreduction. Density functional theory modulations have established a series of transition metal ions incorporated into graphitic carbon nitride catalysts for their catalytic activity toward NO reduction reaction. Among these catalysts, the Cu-based single-atom catalyst showed a limited overpotential of 0.371 V versus reversible hydrogen electrode, effectively suppressing the hydrogen evolution reaction. This improved overall Faradaic efficiency in the NO reduction reaction and enhanced NH_3 production yield. Qi et al. (2022) developed a nanoporous vanadium nitride over carbon foam using a two-step chemical strategy involving hydrothermal treatment followed by high-temperature calcination. This catalyst demonstrated a superior NH_3 production yield rate of 1.05×10^{-7} mol cm^{-2} s^{-1} and a limited overpotential of −0.6 V. In an acidic medium, the catalyst achieved a maximum Faradaic efficiency of 85% versus reversible hydrogen electrode. Furthermore, when tested as a cathode in a Zn–NO battery, the catalyst exhibited a power density of 2 mW cm^{-2}. The vanadium nitride on carbon foam catalysts effectively suppressed the hydrogen evolution reaction, facilitating the hydrogenation and activation of NO, as confirmed through density functional theory calculations. This observation firmly supports the facile fabrication of a catalyst for NO reduction to produce a high yield of NH_3. Niu et al. (Niu et al. 2021) proposed a stable and highly selective Zr–C_2N catalyst for NH_3 production and NO removal using first-principle calculations, which exhibited excellent performance in recent studies. Table 1 summarizes the various transition metal-based electrocatalysts for reducing NO to NH_3.

Prospective

The NO reduction reaction activity toward NH_3 formation is highly influenced by the hydroxylamine formation, which serves as a rate-determining steps for vast ranges of catalysts under different ecological conditions. Therefore, catalysts with improved NO adsorbing ability tend to be highly active and stable. First, achieving maximum selectivity toward the quantified product is crucial for commercial viability. However, the selectivity of these catalysis processes is still unclear owing to the complex branching reaction routes that control selectivity. Qualitative models based on the reaction environment could be attained via NO reduction reaction pathway mechanisms. Especially under acidic and basic

Table 1 Catalytic parameter for the reduction of NO to NH_3 using carbon-incorporated transition metal catalysts

Catalyst	Method	Limited over-potential versus RHE	Power density	Faradaic Efficiency (%)	NH_3 generation rate	References
Nb–SA@B, N–co-doped CNTs	High-temperature annealing	-0.6	–	85.9	8.2×10^{-8} mol cm^{-2} s^{-1}	Peng et al. (2020)
$B_{2.6}$C–TiO$_2$–Ti	Magneto-sputtering	1.55	1.7 mW cm^{-2}	87.6	3678.6 µg h^{-1} cm^{-2}	Liang et al. (2022b)
Co–SA–NC	Two-step chemical strategy	-0.33	1.5	98 ± 0.7	1.43 ± 0.005 mg cm^{-2} h^{-1}	Wu et al. (2021a)
Ni@NC	One-step pyrolysis	0.16	–	72.3	34.6 µmol h^{-1} cm^{-2}	Sethuram Markandaraj et al. (2022)
NiFe–LDH–NSA	One-step hydrothermal	-0.7	1.8	82	112 µmol h^{-1} cm^{-2}	Meng et al. (2022b)
Ag–EDTA–Fe^{2+}	Electrochemical process	-0.165	0.03 kW h^{-1}	100	3.6 mol m^{-2} h^{-1}	Kim et al. (2020)
Fe$_2$O$_3$ on CP	Electrochemical process	-0.45	1.18 mW cm^{-2}	86.73	145.28 µg h^{-1} cm^{-2}	Liang et al. (2022a)
MoS$_2$–GF	Facile chemical process	0.19–0.3	1.04 mW cm^{-2}	76.6	411.8 µg h^{-1} cm^{-2}	Zhang et al. (2021)
MoC@N-doped C	Glucose-assisted pyrolysis	-0.8	1.8 mW cm^{-2}	89 ± 2	1350 ± 15 µg h^{-1} cm^{-2}	Meng et al. (2022a, b)
VN–CF	Two-step chemical process	-0.6	2 mW cm^{-2}	85	1.05×10^{-7} mol cm^{-2} s^{-1}	Qi et al. (2022)
Cu@g–C$_3$N$_4$	DFT modulations	0.371	–	–	–	Wu et al. (2019)

GF graphene felt, *CP* carbon paper, *CNT* carbon nanotube, *CF* carbon foam, *NSA* nanostructure array, *NC* nitrogen-doped carbon, *LDH* layered double hydroxide, *SA* single atom, *RHE* reversible hydrogen electrode, *FE* Faradaic efficiency, *EDTA* ethylenediaminetetraacetate, *VN* vanadium nitride, *DFT* density functional theory

environments, these catalysts tend to exhibit higher selection for NO and NH_3 generation. Owing to the importance of the selectivity of these catalysts in electrocatalytic processes, gaining a deeper insight into how these electrocatalysts could be tailored to exhibit enhanced selectivity toward desired products would be highly beneficial.

Second, a combination of theoretical and experimental analyses enables the identification of acute reaction mechanisms and intermediates involved in the process. In situ characterization techniques, such as Fourier-transform infrared spectroscopy and differential mass spectrometry, can be employed to study the highly reactive intermediates during the NO reduction reaction, providing valuable insights for theoretical modeling. These techniques also aid in determining the effect of different electrochemical environments on the evolution of catalytic materials, allowing for identifying the actual active species of the reaction intermediates through in situ measurements. As a scientific community, researchers engaged in NO reduction reactions face challenges in identifying constant electrolyte conditions and determining area-normalized rates, among other factors, to establish correlations that yield reliable catalytic performance results and achieve consensus on highly active catalysts suitable for specific electrolyte compositions. Henceforth, it is encouraged to

comprehensively analyze a broad range of experimental parameters to evaluate their effects and facilitate extrapolation to diverse electrolyte media. While many studies have focused on the NO reduction reaction activity of noble metals under different pH and NO conditions, it is important to extend these investigations to other transition metal oxides, alloys, and chalcogenides to completely understand the reaction pathways.

Finally, to identify the plausibility of NO reduction reactions in wastewater environments, it is crucial to understand how heavy metals and halide ions limit the catalyst performance. Extensive research has been conducted on various catalytic materials, including metal oxides, alloys, phosphides, and sulfides, to address issues related to electrocatalyst poisoning. Gaining comprehensive insight into the interaction between various pollutant ions and NO on the catalyst surface could lead to examining a new category of materials that possess the selectivity, activity, and stability required for economic NO reduction reaction systems. This valuable information opens numerous opportunities for discovering novel catalyst compounds through computational modulations. To effectively employ this new method, it is essential to cross-check and validate the results through theoretical and experimental measurements. Furthermore, to evaluate their commercial

viability, it is crucial to compare the proposed method with other processes for treating NO, including thermal, chemical, and biological hydrogenation.

Conclusion

Over the last few years, numerous studies have focused on developing electrocatalytic methods for NO reduction and improving NH_3 production. This review provides an overview of progress in developing various electrocatalytic materials for NO reduction and NH_3 generation in aqueous media, suggesting the potential for achieving high NH_3 yields. Nevertheless, there is no agreement on the optimal catalysts required for effective implementation. Hence, scientists must develop an improved rational understanding of materials for NO reduction reaction and establish robust correlations between different electrocatalysts. Electrochemical NO reduction offers a promising approach to convert harmful NO into beneficial NH_3, thereby contributing to a balanced nitrogen cycle. The ideal electrocatalysts for this process are characterized by low cost, great stability, activity, and the selectivity in NH_3 production. However, most current electrocatalysts for NO reduction are metal-bearing and carbon-supported materials. This review discusses the key consideration and operational analyses necessary to understand mechanistic reaction pathways and selective production of products and intermediates. Finally, the review outlines the prospects and challenges in developing an efficient electrochemical process for NO reduction and NH_3 production.

Declarations

Conflict of interest The authors declare no conflict of interest.

References

Anthonysamy SBI, Afandi SB, Khavarian M, Mohamed ARB (2018) A review of carbon-based and non-carbon-based catalyst supports for the selective catalytic reduction of nitric oxide. Beilstein J Nanotechnol 9(1):740–761. https://doi.org/10.3762/bjnano.9.68

Auer E, Freund A, Pietsch J, Tacke T (1998) Carbons as supports for industrial precious metal catalysts. Appl Catal A Gen 173(2):259–271. https://doi.org/10.1016/S0926-860X(98)00184-7

Carro P, Choi J, MacFarlane DR, Simonov AN, Doña-Rodríguez JM, Azofra LM (2022) Competition between metal-catalysed electroreduction of dinitrogen, protons, and nitrogen oxides: a DFT perspective. Catal Sci Technol 12(9):2856–2864. https://doi.org/10.1039/D2CY00389A

Chen K, Shen P, Zhang N, Ma D, Chu K (2023a) Electrocatalytic NO reduction to NH_3 on Mo_2C nanosheets. Inorg Chem 62(2):653–658. https://doi.org/10.1021/acs.inorgchem.2c03714

Chen K, Zhang Y, Xiang J, Zhao X, Li X, Chu K (2023b) p-Block antimony single-atom catalysts for nitric oxide electroreduction to ammonia. ACS Energy Lett 8(3):1281–1288. https://doi.org/10.1021/acsenergylett.2c02882

Clayborne A, Chun H-J, Rankin RB, Greeley J (2015) Elucidation of Pathways for NO Electroreduction on Pt(111) from First Principles. Angewandte Chem Intern Ed 54(28):8255–8258. https://doi.org/10.1002/anie.201502104

de Vooys ACA, Koper MTM, van Santen RA, van Veen JAR (2001) Mechanistic study on the electrocatalytic reduction of nitric oxide on transition-metal electrodes. J Catal 202(2):387–394. https://doi.org/10.1006/jcat.2001.3275

Dorado F, de Lucas-Consuegra A, Jiménez C, Valverde JL (2007) Influence of the reaction temperature on the electrochemical promoted catalytic behaviour of platinum impregnated catalysts for the reduction of nitrogen oxides under lean burn conditions. Appl Catal A Gen 321(1):86–92. https://doi.org/10.1016/j.apcata.2007.01.035

Esrafili MD, Arjomandi Rad F (2019) Carbon-doped boron nitride nanosheets as highly sensitive materials for detection of toxic NO and NO_2 gases: a DFT study. Vacuum 166:127–134. https://doi.org/10.1016/j.vacuum.2019.04.065

Fan Y, Xue X, Zhu L, Qin Y, Yuan D, Gu D, Wang B (2023) The state-of-the-art in the electroreduction of NO_x for the production of ammonia in aqueous and nonaqueous media at ambient conditions: a review. New J Chem 47(13):6018–6040. https://doi.org/10.1039/D2NJ06362J

Fu X, Zhang J, Kang Y (2022) Recent advances and challenges of electrochemical ammonia synthesis. Chem Catal 2(10):2590–2613. https://doi.org/10.1016/j.checat.2022.09.001

He C, Shi P, Pang D, Zhang Z, Lin L (2022) Design of S-vacancy FeS_2 as an electrocatalyst for NO reduction reaction: a DFT study. Mol Catal. https://doi.org/10.1016/j.mcat.2022.112327

He C, Wang J, Fu L, Zhao C, Huo J (2022) Associative vs. dissociative mechanism: electrocatalysis of nitric oxide to ammonia. Chin Chem Lett 33(2): 1051–1057 https://doi.org/10.1016/j.cclet.2021.09.009

Jiang Q, Li T, He Y, Wu Y, Zhang J, Jiang M (2022) Simultaneous removal of hydrogen sulfide and ammonia in the gas phase: a review. Environ Chem Lett 20(2):1403–1419. https://doi.org/10.1007/s10311-021-01366-w

Kim D, Shin D, Heo J, Lim H, Lim J-A, Jeong HM, Kim B-S, Heo I, Oh I, Lee B, Sharma M, Lim H, Kim H, Kwon Y (2020) Unveiling electrode-electrolyte design-based NO reduction for NH_3 synthesis. ACS Energy Lett 5(11):3647–3656. https://doi.org/10.1021/acsenergylett.0c02082

Kim DH, Ringe S, Kim H, Kim S, Kim B, Bae G, Oh H-S, Jaouen F, Kim W, Kim H, Choi CH (2021) Selective electrochemical reduction of nitric oxide to hydroxylamine by atomically dispersed iron catalyst. Nat Commun 12(1):1856. https://doi.org/10.1038/s41467-021-22147-7

Ko BH, Hasa B, Shin H, Zhao Y, Jiao F (2022) Electrochemical reduction of gaseous nitrogen oxides on transition metals at ambient conditions. J Am Chem Soc 144(3):1258–1266. https://doi.org/10.1021/jacs.1c10535

Kwon Y-i, Kim SK, Kim YB, Son SJ, Nam GD, Park HJ, Cho W-C, Yoon HC, Joo JH (2021) Nitric oxide utilization for ammonia production using solid electrolysis cell at atmospheric pressure. ACS Energy Lett 6(12):4165–4172. https://doi.org/10.1021/acsenergylett.1c01972

Lang Z, Miao J, Tan H, Su Z, Li Y, Zheng Z (2020) Element table of TM-substituted polyoxotungstates for direct electrocatalytic reduction of nitric oxide to ammonia: a DFT guideline for experiments. Inorg Chem Front 7(22):4507–4516. https://doi.org/10.1039/D0QI01014F

Lee SJ, Theerthagiri J, Nithyadharseni P, Arunachalam P, Balaji D, Madan Kumar A, Madhavan J, Mittal V, Choi MY (2021) Heteroatom-doped graphene-based materials for sustainable energy applications: a review. Renew Sustain Energy Rev https://doi.org/10.1016/j.rser.2021.110849

Li C, Yang J, Zhang L, Li S, Yuan Y, Xiao X, Fan X, Song C (2021) Carbon-based membrane materials and applications in water and wastewater treatment: a review. Environ Chem Lett 19(2):1457–1475. https://doi.org/10.1007/s10311-020-01112-8

Li Y, Nie J, Gao D, Zhao S, Zhang Y, Bian B, Guo Z, Huang Y, Fang Y, Tang C (2023) Hexagonal boron nitride nanoribbon as a novel metal-free catalyst for high-efficiency NO reduction to NH_3. Fuel https://doi.org/10.1016/j.fuel.2022.126943

Liang J, Chen H, Mou T, Zhang L, Lin Y, Yue L, Luo Y, Liu Q, Li N, Alshehri AA, Shakir I, Agboola PO, Wang Y, Tang B, Ma D, Sun X (2022a) Coupling denitrification and ammonia synthesis via selective electrochemical reduction of nitric oxide over Fe_2O_3 nanorods. J Mater Chem A 10(12):6454–6462. https://doi.org/10.1039/D2TA00744D

Liang J, Liu P, Li Q, Li T, Yue L, Luo Y, Liu Q, Li N, Tang B, Alshehri AA, Shakir I, Agboola PO, Sun C, Sun X (2022) Amorphous boron carbide on titanium dioxide nanobelt arrays for high-efficiency electrocatalytic NO reduction to NH_3. Angewandte Chem Int Ed. https://doi.org/10.1002/anie.202202087

Liu S, Liu Y, Cheng Z, Gao X, Tan Y, Shen Z, Yuan T (2021) Two-dimensional transition metal phthalocyanine sheet as a promising electrocatalyst for nitric oxide reduction: a first principle study. Environ Sci Pollut Res 28(6):7191–7199. https://doi.org/10.1007/s11356-020-11058-7

Long J, Chen S, Zhang Y, Guo C, Fu X, Deng D, Xiao J (2020) Direct Electrochemical ammonia synthesis from nitric oxide. Angewandte Chem Int Ed 59(24):9711–9718. https://doi.org/10.1002/anie.202002337

Long J, Guo C, Fu X, Jing H, Qin G, Li H, Xiao J (2021) Unveiling potential dependence in NO electroreduction to ammonia. J Phys Chem Lett 12(29):6988–6995. https://doi.org/10.1021/acs.jpclett.1c01691

Long J, Li H, Xiao J (2023) The progresses in electrochemical reverse artificial nitrogen cycle. Curr Opin Electrochem. https://doi.org/10.1016/j.coelec.2022.101179

Meng G, Jin M, Wei T, Liu Q, Zhang S, Peng X, Luo J, Liu X (2022a) MoC nanocrystals confined in N-doped carbon nanosheets toward highly selective electrocatalytic nitric oxide reduction to ammonia. Nano Res 15(10):8890–8896. https://doi.org/10.1007/s12274-022-4747-y

Meng G, Wei T, Liu W, Li W, Zhang S, Liu W, Liu Q, Bao H, Luo J, Liu X (2022b) NiFe layered double hydroxide nanosheet array for high-efficiency electrocatalytic reduction of nitric oxide to ammonia. Chem Commun 58(58):8097–8100. https://doi.org/10.1039/D2CC02463B

Mokhtar NAIM, Zawawi RM, Khairul WM, Yusof NA (2022) Electrochemical and optical sensors made of composites of metal–organic frameworks and carbon-based materials. Rev Environ Chem Lett 20(5):3099–3131. https://doi.org/10.1007/s10311-022-01403-2

Mudchimo T, Namuangruk S, Kungwan N, Jungsuttiwong S (2018) Carbon-doped boron nitride nanosheet as a promising metal-free catalyst for NO reduction: DFT mechanistic study. Appl Catal A Gen 557:79–88. https://doi.org/10.1016/j.apcata.2018.02.025

Muradov N, Smith F, Raissi TA (2005) Catalytic activity of carbons for methane decomposition reaction. Catal Today 102–103:225–233. https://doi.org/10.1016/j.cattod.2005.02.018

Naik SS, Theerthagiri J, Lee SJ, Yu Y, Choi MY (2022) Multiscale design of 3D metal–organic frameworks (M−BTC, M: Cu, Co, Ni) via PLAL enabling bifunctional electrocatalysts for robust overall water splitting. Chem Eng J. https://doi.org/10.1016/j.cej.2022.137045

Niu H, Zhang Z, Wang X, Wan X, Kuai C, Guo Y (2021) A Feasible strategy for identifying single-atom catalysts toward electrochemical NO-to-NH_3 conversion. Small. https://doi.org/10.1002/smll.202102396

Ouyang L, Zhou Q, Liang J, Zhang L, Yue L, Li Z, Li J, Luo Y, Liu Q, Li N, Tang B, Ali Alshehri A, Gong F, Sun X (2022) High-efficiency NO electroreduction to NH_3 over honeycomb carbon nanofiber at ambient conditions. J Coll Int Sc 616:261–267. https://doi.org/10.1016/j.jcis.2022.02.074

Peng X, Mi Y, Bao H, Liu Y, Qi D, Qiu Y, Zhuo L, Zhao S, Sun J, Tang X, Luo J, Liu X (2020) Ambient electrosynthesis of ammonia with efficient denitration. Nano Energy https://doi.org/10.1016/j.nanoen.2020.105321

Qi D, Lv F, Wei T, Jin M, Meng G, Zhang S, Liu Q, Liu W, Ma D, Hamdy MS, Luo J, Liu X (2022) High-efficiency electrocatalytic NO reduction to NH_3 by nanoporous VN. Nano Res Energy. https://doi.org/10.26599/NRE.2022.9120022

Ren Z, Zhang H, Wang S, Huang B, Dai Y, Wei W (2022) Nitric oxide reduction reaction for efficient ammonia synthesis on topological nodal-line semimetal Cu_2Si monolayer. J Mater Chem A 10(15):8568–8577. https://doi.org/10.1039/D2TA00504B

Rodríguez-reinoso F (1998) The role of carbon materials in heterogeneous catalysis. Carbon 36(3):159–175. https://doi.org/10.1016/S0008-6223(97)00173-5

Rosca V, Duca M, de Groot MT, Koper MTM (2009) Nitrogen cycle electrocatalysis. Chem Rev 109(6):2209–2244. https://doi.org/10.1021/cr8003696

Saeidi N, Esrafili MD (2023) Boron-embedded C_3N nanosheets as efficient electrocatalysts for reduction of nitric oxide. Int J Hydrogen Energy 48(51):19509–19521. https://doi.org/10.1016/j.ijhydene.2023.02.052

Saeidi N, Esrafili MD, Sardroodi JJ (2021) NO electrochemical reduction over $Si–N_4$ embedded graphene: a DFT investigation. Appl Surf Sci. https://doi.org/10.1016/j.apsusc.2020.148869

Sethuram Markandaraj S, Muthusamy T, Shanmugam S (2022) Electrochemical reduction of nitric oxide with 1.7% solar-to-ammonia efficiency over nanostructured core-shell catalyst at low overpotentials. Adv Sci 9(29):2201410. https://doi.org/10.1002/advs.202201410

Shahid UB, Siddharth K, Shao M (2021) Electrifying the nitrogen cycle: an electrochemical endeavor. Curr Opin Electrochem. https://doi.org/10.1016/j.coelec.2021.100790

Shrestha KP, Seidel L, Zeuch T, Mauss F (2018) Detailed kinetic mechanism for the oxidation of ammonia including the formation and reduction of nitrogen oxides. Energy Fuels 32(10):10202–10217. https://doi.org/10.1021/acs.energyfuels.8b01056

Soto-Hernández J, Santiago-Ramirez CR, Ramirez-Meneses E, Luna-Trujillo M, Wang J-A, Lartundo-Rojas L, Manzo-Robledo A (2019) Electrochemical reduction of NO_x species at the interface of nanostructured Pd and PdCu catalysts in alkaline

conditions. Appl Catal B Environ. https://doi.org/10.1016/j.apcatb.2019.118048

Stüber F, Font J, Fortuny A, Bengoa C, Eftaxias A, Fabregat A (2005) Carbon materials and catalytic wet air oxidation of organic pollutants in wastewater. Top Catal 33(1):3–50. https://doi.org/10.1007/s11244-005-2497-1

Teng H, Suuberg EM, Calo JM (1992) Studies on the reduction of nitric oxide by carbon: the nitric oxide-carbon gasification reaction. Energy Fuels 6(4):398–406. https://doi.org/10.1021/ef00034a008

Theerthagiri J, Karuppasamy K, Park J, Rahamathulla N, Kumari MLA, Souza MKR, Cardoso ESF, Murthy AP, Maia G, Kim H-S, Choi MY (2022a) Electrochemical conversion of biomass-derived aldehydes into fine chemicals and hydrogen: a review. Environ Chem Lett. https://doi.org/10.1007/s10311-022-01543-5

Theerthagiri J, Lee SJ, Murthy AP, Madhavan J, Choi MY (2020) Fundamental aspects and recent advances in transition metal nitrides as electrocatalysts for hydrogen evolution reaction: a review. Curr Opin Solid State Mater Sci. https://doi.org/10.1016/j.cossms.2020.100805

Theerthagiri J, Murthy AP, Lee SJ, Karuppasamy K, Arumugam SR, Yu Y, Hanafiah MM, Kim H-S, Mittal V, Choi MY (2021) Recent progress on synthetic strategies and applications of transition metal phosphides in energy storage and conversion. Ceramics Int 47(4):4404–4425. https://doi.org/10.1016/j.ceramint.2020.10.098

Theerthagiri J, Park J, Das HT, Rahamathulla N, Cardoso ESF, Murthy AP, Maia G, Vo DVN, Choi MY (2022b) Electrocatalytic conversion of nitrate waste into ammonia: a review. Environ Chem Lett. https://doi.org/10.1007/s10311-022-01469-y

Toth JE, Anson FC (1989) Electrocatalytic reduction of nitrite and nitric oxide to ammonia with iron-substituted polyoxotungstates. J Am Chem Soc 111(7):2444–2451. https://doi.org/10.1021/ja00189a012

Wan H, Bagger A, Rossmeisl J (2021) Electrochemical nitric oxide reduction on metal surfaces. Angewandte Chem Int Ed 60(40):21966–21972. https://doi.org/10.1002/anie.202108575

Wang J, Li K, Hao Q, Liu D, Zhang X (2023) Electroreduction NO to NH_3 over single metal atom anchored on pyrrole type defective graphene: a DFT study. Chin Chem Lett https://doi.org/10.1016/j.cclet.2022.05.081

Wang Z, Zhao J, Wang J, Cabrera CR, Chen Z (2018) A Co–N_4 moiety embedded into graphene as an efficient single-atom-catalyst for NO electrochemical reduction: a computational study. J Mater Chem A 6(17):7547–7556. https://doi.org/10.1039/C8TA00875B

Werchmeister RML, Hansen KK (2013) Electrochemical reduction of oxygen and nitric oxide at low temperature on $Ce_{1-x}Pr_xO_{2-\delta}$ cathodes. Electrochimica Acta 114:474–477. https://doi.org/10.1016/j.electacta.2013.10.056

Wu A, Yang J, Xu B, Wu X-Y, Wang Y, Lv X, Ma Y, Xu A, Zheng J, Tan Q, Peng Y, Qi Z, Qi H, Li J, Wang Y, Harding J, Tu X, Wang A, Yan J, Li X (2021) Direct ammonia synthesis from the air via gliding arc plasma integrated with single atom electrocatalysis. Appl Catal B Environ. https://doi.org/10.1016/j.apcatb.2021.120667

Wu J, Yu Y-X (2023) Efficient electrocatalysts refined from metal-dimer-anchored PC6 monolayers for NO reduction to ammonia.

Int J Hydrogen Energy 48(15):5961–5975. https://doi.org/10.1016/j.ijhydene.2022.11.180

Wu Q, Wang H, Shen S, Huang B, Dai Y, Ma Y (2021b) Efficient nitric oxide reduction to ammonia on a metal-free electrocatalyst. J Mater Chem A 9(9):5434–5441. https://doi.org/10.1039/D0TA11209G

Wu Q, Wei W, Lv X, Wang Y, Huang B, Dai Y (2019) Cu@g-C_3N_4: an efficient single-atom electrocatalyst for NO electrochemical reduction with suppressed hydrogen evolution. J Phys Chem C 123(51):31043–31049. https://doi.org/10.1021/acs.jpcc.9b08827

Xia D, Yu H, Li H, Huang P, Li Q, Wang Y (2022) Carbon-based and carbon-supported nanomaterials for the catalytic conversion of biomass: a review. Environ Chem Lett 20(3):1719–1744. https://doi.org/10.1007/s10311-022-01402-3

Xiao Y, Shen C (2021) Transition-metal borides (MBenes) as new high-efficiency catalysts for nitric oxide electroreduction to ammonia by a high-throughput approach. Small 17(24):2100776. https://doi.org/10.1002/smll.202100776

Yu Y, Lee SJ, Theerthagiri J, Fonseca S, Pinto LMC, Maia G, Choi MY (2022) Reconciling of experimental and theoretical insights on the electroactive behavior of C/Ni nanoparticles with AuPt alloys for hydrogen evolution efficiency and non-enzymatic sensor. Chem Eng J. https://doi.org/10.1016/j.cej.2022.134790

Zang Y, Wu Q, Wang S, Huang B, Dai Y, Ma Y (2023) Activating dual atomic electrocatalysts for the nitric oxide reduction reaction through the P/S element. Mater Horiz. https://doi.org/10.1039/D2MH01440H

Zhang G, Wan Y, Zhao H, Guo Y, Chu K (2023) A metal-free catalyst for electrocatalytic NO reduction to NH_3. Dalton Trans 52(19):6248–6253. https://doi.org/10.1039/D3DT00994G

Zhang L, Liang J, Wang Y, Mou T, Lin Y, Yue L, Li T, Liu Q, Luo Y, Li N, Tang B, Liu Y, Gao S, Alshehri AA, Guo X, Ma D, Sun X (2021) High-performance electrochemical NO reduction into NH_3 by MoS_2 nanosheet. Angewandte Chem Int Ed 60(48):25263–25268. https://doi.org/10.1002/anie.202110879

Zhao S, Lu X, Wang L, Gale J, Amal R (2019) Carbon-based metal-free catalysts for electrocatalytic reduction of nitrogen for synthesis of ammonia at ambient conditions. Adv Mater 31(13):1805367. https://doi.org/10.1002/adma.201805367

Zhao Y, Yan L, Zhao X (2022) Development of carbon-based electrocatalysts for ambient nitrogen reduction reaction: challenges and perspectives. Chem Electro Chem. https://doi.org/10.1002/celc.202101126

Zhou Q, Gong F, Xie Y, Xia D, Hu Z, Wang S, Liu L, Xiao R (2022) A general strategy for designing metal-free catalysts for highly-efficient nitric oxide reduction to ammonia. Fuel. https://doi.org/10.1016/j.fuel.2021.122442